MASS TRANSFER OF DIALYZABLE CONSTITUENTS DURING HEMODIALYSIS OF UREMIC PATIENTS

by

GORDON CARL PAGE, B.S. in Ch.E., M.S. in Ch.E.

A DISSERTATION

IN

CHEMICAL ENGINEERING

Submitted to the Graduate Faculty
of Texas Tech University in
Partial Fulfillment of
the Requirements for
the Degree of

DOCTOR OF PHILOSOPHY

August, 1975

ACKNOWLEDGEMENTS

The following acknowledgements are directed to the persons and institutions which directly aided in the successful completion of this investigation:

1. Mr. Herbert Janssen for sample collection and analysis.
2. Mrs. Irene Bradley for sample collection and analysis.
3. Mr. Steve Gibbon for sample analysis.
4. Dr. G. F. Meenaghan for his support and advice.
5. Dr. L. J. O'Brien for his support and advice.
6. The South Plains Dialysis Center for the experimental subjects and valuable suggestions.
7. The Department of Physiology for their valuable suggestions and partial funding.
8. The 3M Company for partial funding.
9. The Texas Tech University Institute for University Research for partial funding.

TABLE OF CONTENTS

LIST OF TABLES

LIST OF FIGURES

CHAPTER 1

INTRODUCTION

The uremic syndrome results from the retention of normal and abnormal metabolic end-products associated with kidney disease. The basic clinical characteristics of uremia have been known for over one hundred years. Until recently, uremia meant a hopeless prognosis; however, now a uremic patient can undergo hemodialysis therapy and can lead a relatively useful and productive life.

There are, however, metabolic problems which occur in uremic patients because of inadequate dialysis of uremic toxins (5, 40). In order to insure adequate removal of these toxins, mathematical models describing hemodialysis have been proposed (4, 5, 52, 54, 55). These models were developed to predict the dialysis time and hemodialyzer operating conditions required to achieve adequate dialysis. In verifying these models, researchers have been severely limited to the number of dialyzed constituents that could be monitored during hemodialysis therapy. This limitation was overcome in this investigation by incorporating high pressure, anion-exchange chromatography to monitor the change in concentration of forty-four dialyzed constituents during hemodialysis.

A general mathematical model was to be developed in this investigation to predict the dialysis time and hemodialyzer operating conditions required to remove a specified fraction of a dialyzable constituent from the body fluids. The development of this model

was to be verified from the change in concentration of the monitored constituents during the hemodialysis treatment. The model variables which affect the mass transfer of dialyzable components were also to be determined and correlated to measurable parameters. Once achieving these objectives, this model could then be used as a basis for the development of treatment programs for uremic patients undergoing hemodialysis therapy.

CHAPTER 2

THE KIDNEY AS A HEMOSTATIC ORGAN

The human kidney is comprised of approximately one million functioning units called nephrons. The physiological portions of a nephron, shown in Figure 1, consist of a Bowman's capsule which surrounds a network of capillaries called the glomerular tuft, and a tubule composed of a proximal portion, Henle's loop, and a distal portion which drains into a collecting duct. The capsule, proximal tubule, and distal tubule are found in the renal cortex. The loop of Henle and most of the collecting duct are in the renal medulla.

The nephron performs two basic functions which are essential for life. First, the nephron regulates the volume and composition of the body fluids. For example, it conserves water and essential substances and maintains the body fluid's acid-base balance. Second, the nephron removes noxious, foreign, and nonessential components from the body fluid. These functions are carried out by three mechanisms: filtration, reabsorption, and secretion.

Filtration of the blood occurs at the glomerulus. The filtration does not directly require expenditure of metabolic energy, but depends on the effective filtration pressure across the glomerular membrane. This pressure forces a protein-free filtrate of plasma through this membrane.

Since the normal glomerular filtration rate in an adult male is approximately 125 ml/min (50) or 180 liters per day, most of

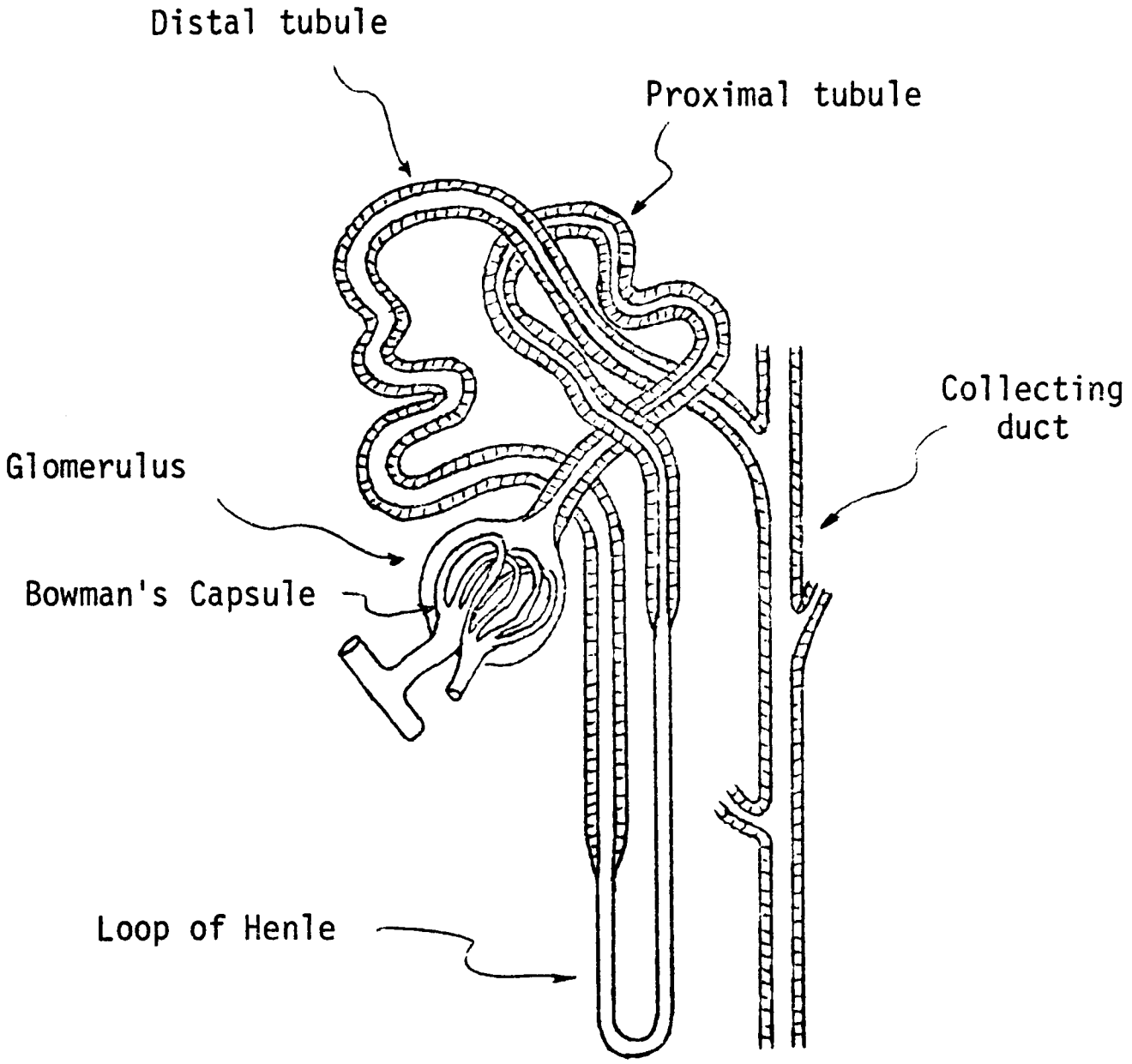

Figure 1. Schematic of the physiological portions of a nephron.

this filtrate must be reabsorbed back into the body fluids. This reabsorption occurs in the proximal and distal tubules, the loop of Henle, and the collecting duct with approximately 80% of the glomerular filtrate being reabsorbed in the proximal tubule. The various types of reabsorption mechanisms can be divided into (a) active transport which involves reabsorption exhibiting a transport maxima or a gradient-time limitation and requires metabolic energy and (b) passive transport which requires an osmotic or electrochemical gradient.

Tubular secretion resembles tubular reabsorption in that active secretion exhibits a transport maxima or a gradient-time limitation and passive secretion occurs across a gradient. Tubular secretion is very important because it is the mechanism whereby protein-bound drugs and metabolites are removed from the body fluid (50).

In order to regulate the levels of metabolic end-products and the body fluid volume and composition, it is necessary for the kidney to correctly perform all of its functions. If any of these functions are destroyed, pathological disturbances throughout the entire body will occur.

CHAPTER 3

CAUSES OF CHRONIC RENAL FAILURE

Renal failure can be caused by various pathologic disorders (51). These disorders include, glomerulonephritis, pyelonephritis, lipid nephrosis, tubular necrosis, nephrosclerosis, and congenital disorders such as polycystic disease.

Glomerulonephritis is an inflammatory disease afflicting the glomerular capillary tuft. As this disease progresses, it will eventually affect all the elements of the nephron. Fibrosis with total destruction of the glomeruli is accompanied by degeneration of the tubules. In the end-stage of chronic glomerulonephritis, the kidney is reduced to a shriveled, contracted mass of scar tissue.

Pyelonephritis is a manifestation of bacterial infection of the kidneys. This disease is patchy in distribution with variable severity throughout the kidney. In the end-stage, pyelonephritis has the same characteristics as glomerulonephritis.

Tubular necrosis is usually caused by nephrotoxic compounds such as dichlorides of mercury or carbon tetrachloride or by prolonged ischemia and anoxia. The nephrotoxic agents usually first attack the proximal tubule. Ischemia can affect any part of the kidney. Initially, this disease results in acute renal failure with a rapid development of uremia.

Nephrosclerosis can either be benign or malignant. Benign nephrosclerosis is associated with essential hypertension with spotty scaring of the renal tissue. Malignant nephrosclerosis is a form of hypertension with features characterized by rapidly progressing renal insufficiency. It ultimately leads to chronic renal failure.

Congenital polycystic disease is perhaps the most common structural renal disorder (51). This disorder occurs when there is widespread failure of the union between glomerular and tubular anlagen. This disorder may not be detected until the third or fourth decade of life. Other inborn renal defects include, nephrogenic diabetes insipides, acidosis, renal hyper- and hypophosphatemia, and essential hypertension. All of these defects usually lead to chronic renal failure.

Renal disease causing uremia can thus affect the glomerular capillary tuft, the activity of one or all the segments in the renal tubules or the adequacy of blood perfusion of the renal parenchyma. As each of these diseases progresses, their symptoms ultimately converge into a common pattern of absolute renal insufficiency with death in uremia.

CHAPTER 4

BIOCHEMICAL CHARACTERISTICS OF CHRONIC RENAL FAILURE

Many mechanisms have been proposed to explain the toxic symptoms of uremia. These proposed mechanisms generally conclude that uremia is caused by an accumulation of metabolic products either working alone or in combination to affect metabolic pathways by some modification of enzymatic reactions.

Urea

One of the first components which was found to be related to uremia was urea (8, 10). Urea is normally formed only in the liver as one of the end-products of protein catabolism. In acute renal failure, there is a significant correlation (70) between the severity of the kidney disease and blood urea concentration. In chronic renal failure, this relationship does not hold true, especially if the patient is on a low protein diet. In 1968, Pitts (51) stated that when urea was administered to normal subjects in amounts sufficient to achieve blood urea levels comparable to those found in chronic renal failure, the subjects suffered only from thirst and polyuria and exhibited none of the other manifestations of uremia. The work of Merrill, et al. (43) also showed that a high urea blood concentration by itself had little or no effect in causing symptoms of uremia. These investigators hemodialyzed patients with chronic renal failure using dailysate fluid containing a high urea concen-

tration. They noted that despite the high blood urea levels, these patients had excellent clinical responses to the dialysis treatments. Other investigators, however, report that urea does indeed play a toxic role in uremia. Grollman and Grollman (31) reported that at extremely high blood urea concentrations, 540 to 1690 mg%, (mg/100 ml), experimental dogs exhibited severe uremic symptoms. These symptoms included weakness and anorexia followed by vomiting and diarrhea which terminated in bowel hemorrhage and coma. These observations could possibly be caused by changes in intracellular water and electrolyte concentrations. There is also evidence that urea acts as an enzyme inhibitor.

Guanidine and Other Organic Components

Though there is conflicting evidence whether urea by itself does or does not cause uremic symptoms, it is generally accepted that the major cause of the symptoms in end-stage renal failure is the end-products of protein catabolism. It is also believed that certain intermediate breakdown products accumulate in the body and contribute to symptoms of uremia. In 1915, Foster (26) reported that he had isolated an organic base from uremic blood which caused immediate symptoms of uremia when injected into guinea pigs. These initial symptoms were rapid breathing and muscular twitching followed by convulsions and ending in death. This isolated substance was later shown (33) to be guanidine or a guanidine derivitive. Other substances (42, 46) have also been implicated with uremia. These include

creatinine, potassium, nephrolysins, and phenols. After these discoveries, it was and still is accepted that uremic symptoms are not caused by only one substance but by a number of toxic metabolic components which accumulate in the body.

To date, the organic compounds reported to accumulate in the body include: urea, creatinine, creatine, uric acid, various amino acids and polypeptides, indican, hippuric acid, phenol conjugates, phenolic and indolic acids and their conjugates, organic acids of the tricarboxylic acid cycle, guanidine bases, acetoin and 2, 3, butylene glycol (15, 38, 46, 62, 65, 67). Of these uremic compounds, the excesses of polypeptides and guanidine bases were uncertain due to separation techniques. Because of the recent advances made in these techniques, many workers (9, 32, 41, 47) have reported that indeed there is an increase in various polypeptides and guanidine bases in uremic patients, and that the concentration of these components is especially high in the cerebrospinal fluid (62). It would thus seem possible that these compounds could diffuse into the brain and other tissues causing symptoms of chronic renal failure.

Because of the recent interest in guanidine related compounds as a uremic toxic factor, various researchers have postulated different mechanisms which could relate uremic symptoms to guanidine compounds. For example, Cohen, et al. (16) postulated that due to increased nitrogen retention, there is an alternate pathway involved in ammonia detoxification and urea synthesis. This mechanism would involve the inhibition of normal enzyme activity and cause either

the activation of a dormant enzyme or the creation of a new enzyme. Increased quantities of serum and cerebrospinal guanidinosuccinic acid in uremic patients were confirmed by Stein, et al. (64). Also, Giovanetti, et al. (29) reported that methylguanidine, a constituent of creatinine, was present in uremic body fluids and that it accounted for almost all the mono-substituted guanidines which accumulate in chronic renal failure.

Mason et al. (42) first demonstrated the toxic role of guanidine in uremia. They felt, however, that due to the crude separation techniques available, they could not be certain that this substance played a definite role in uremic symptoms. It was not until 1969 that guanidine compounds were shown to definitely cause symptoms of uremia. Giovanetti, et al. (28) injected experimental dogs with toxic amounts of methylguanidine. These test animals first exhibited a decrease in body weight at a rate which implied that methylguanidine exerted a protein catabolic effect. The dogs then showed gastro-intestinal tract distrubances, cardiovascular and respiratory abnormalities and disturbances of the central and peripheral nervous system. The potentially important role of guanidines in the causes of symptoms of uremia is still the subject of much research and awaits results of further studies.

Enzyme Inhibition

There is also the possibility that retained metabolic substances in uremia may cause an inhibition of enzymes of metabolic reactions.

The effect of urea on monoamine oxidase (27) is quite pronounced. The activity of monoamine oxidase decreases with an increase of urea till a maximum inhibition is reached. At this point, the enzyme activity begins increasing as urea concentration increases. Substances other than urea have also been investigated as enzyme inhibitors. The effect of phenolic acids (34) on cerebral metabolism was studied by Hicks, et al. They determined this effect by measuring the respiration rate and anaerobic glycolysis of guinea pig brain slices and the inhibition of selected enzymes involved in the cerebral metabolism. They showed that many aromatic acids, especially those with an unsaturated side chain, inhibited the enzyme reaction rates. It should be noted that the levels of phenolic acids used by Hicks were higher than reported values (57) in uremic plasma. In light of this, Hicks suggested that the lower plasma levels of phenolic acids in uremic body fluids could possibly exert the same effect as the high amounts used by being present for a long period of time. It is also possible that the retained phenolic acids could exert an enzyme inhibitory action by a summation effect in vivo. Enzyme inhibition by aromatic and aliphatic amines has also been shown (70). Compared to phenolic acids, these amines were less effective inhibitors of glutamic acid and dihydroxyphenylalanine decarboxylases. It should be noted that these amines cross the blood-brain barrier more readily than the phenolic acids (58), thus these amines could be much more effective in vivo than the aromatic acids. In 1971, Quadricci, et al. (53), studied the effect of uremic serum on skin cell growth. They

showed that there was a marked decrease in skin cell growth and that urea and creatinine did not effect the growth of skin cells. Experiments were also made using serum from a well dialyzed patient and a poorly dialyzed patient. The serum taken from the well dialyzed patient was shown to support cellular growth better than the serum from the poorly dialyzed patient. These experiments imply that components other than urea or creatinine inhibit enzymes involved in skin cell growth. The effect of uremic body fluids on transketolase activity (TKA) has also been investigated (5, 55). The basis for studying TKA in uremia was because a degeneration of myeline sheaths has been found as a morphologic lesion underlying the periphral neuropathy of chronic renal failure (3, 18), and the metabolism of myeline sheath maintenance has been proposed to require an intact pentose-phosphate shunt. In this metabolic pathway, transketolase has an important function (22). In 1970, Ramos, et al. (55) reported that patients who have been adequately dialyzed on the basis of small molecules such as urea, uric acid, and creatinine have contracted neuropathy. It was also reported by Lonergan and associates (41) that uremic compounds having a molecular weight less than 500 had a marked effect on inhibiting TKA. Uremic compounds having a molecular weight over 500 did not exhibit this inhibitory effect. He also found that guanidinosuccinic acid which is contained in uremic body fluids inhibited TKA similar to uremic serum.

Uric Acid

Another feature of chronic renal failure is a marked increase in the plasma concentration of uric acid. It has been observed that rarely does hyperuricema result in classical gout. In 1968, Richet (56) suggested that due to the infrequent occurance of gout in uremic patients, the uric acid metabolism is different from that of normal subjects. They proposed that uricolysis was an important factor in this situation. Sorenson (63) reported that the extrarenal elimination of uric acid occurs entirely in the gastrointestinal tract and is catalyzed by bacterial enzymes. He suggested that this uricolysis becomes increasingly important as the uric acid concentration increases.

Oxalic Acid

The retention of oxalic acid (71) and crystal deposition in both the myocardium and renal tissues has been reported as a complication of chronic renal failure (6, 7, 25). There is evidence (23, 24) that oxalic acid also inhibits lactic dehydrogenase. The role of oxalic acid retention in chronic renal failure still remains uncertain.

The abnormalities of metabolism caused by chronic renal failure constitute a major problem in medical research. To date, little is known about the body fluid constituents which cause the symptoms of chronic uremia. Thus, to completely understand the uremic syndrome, it is imperative that these uremic toxins be known.

CHAPTER 5

HEMODIALYSIS AS A TREATMENT FOR UREMIA

In 1913, Able, Rowntree, and Turner (1) developed the first artificial kidney and used it in a series of experiments on dogs. These researchers suggested that this procedure could be used to remove toxic components of patients afflicted with uremia. The first clinical use of hemodialysis as a treatment for uremia was described by Kloff and Berk in 1944 (34). Today, hemodialysis is an accepted technique for treating patients suffering from chronic renal failure.

Figure 2 is a schematic of a typical hemodialysis system. Arterial blood is pumped from the patient into the Cordis Dow Artificial Kidney (CDAK). In the artifical kidney, body-fluid constituents are removed by two distinct mechanisms, diffusion and ultrafiltration across a semipermeable membrane. The driving force for diffusion is a concentration gradient across the membrane, and the driving force for ultrafiltration is a hydrostatic pressure gradient across the membrane. After passing through the aftificial kidney, the dialyzed blood is returned to the patient's venous system. The fluid that removes the dialyzed constituents from the artificial kidney is called the dialysate. This fluid flows on the outside of the kidney's semipermeable membrane. Since the dialysate pump is located after the artificial kidney, the dialysate side can operate at subatmospheric pressures, thereby, increasing the ultrafiltration pressure gradient. The dialysate flow can either be single pass or

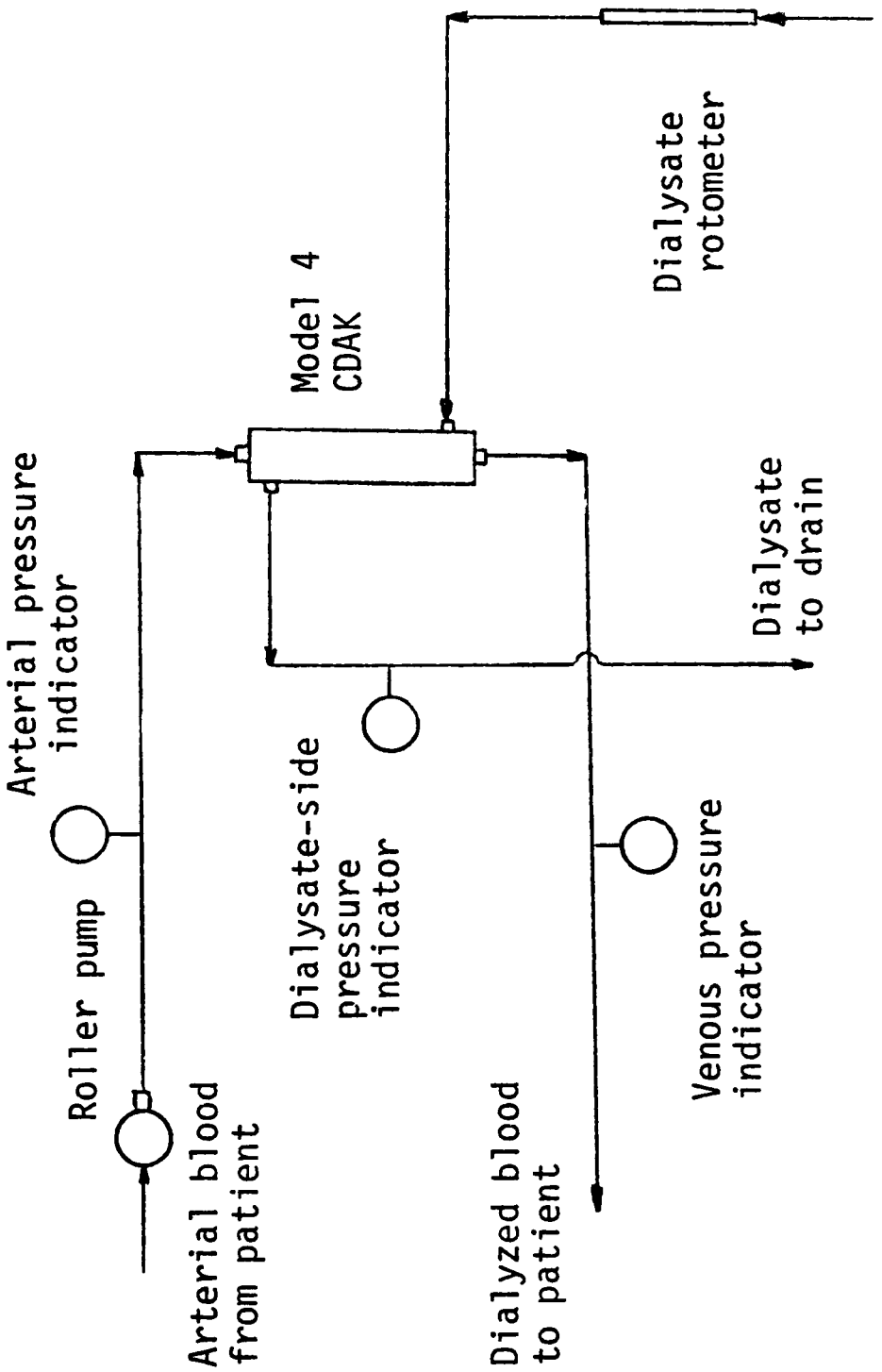

Figure 2. Schematic of a typical hemodialysis system.

recirculated. Table 1 shows a typical composition of a dialysate fluid. It is necessary for the dialysate to have these components to insure that the body fluid is not depleted of electrolytes or sugar during the course of hemodialysis. This composition can also be modified depending on the specific end to be achieved. For example, in hyperkalemia, potassium concentration would be reduced or eliminated in the dialysate. If alkalosis exists, the sodium acetate concentration would be reduced and the chloride concentration increased.

There are at least two main problems associated with using an artificial kidney to remove constituents from the body fluid. First, the semipermeable membranes do not allow the passage of proteins (66) and the removal of "middle molecules" having an apparent molecular weight over 500 is slow (30). This means that drugs and metabolic end-products which are bound to proteins cannot be adequately removed by hemodialysis therapy. Also, the time required to remove "middle molecules" from the body fluid is long. This problem is exemplified by various neuropathic disorders occuring in poorly dialyzed, uremic patients (5, 41, 55). The second problem associated with hemodialysis is the depletion of essential substances such as amino acids from the body fluid during dialysis. According to Alfrey, et al. (2), uremic patients have died of encephalopathy even though their dialysis times were increased.

Today, a patient afflicted with chronic renal failure can undergo hemodialysis therapy and can lead a relatively useful and pro-

TABLE 1

COMPOSITION OF A TYPICAL DIALYSATE

Component	Concentration (g/l)
$CaCl_3 \cdot 2H_2O$	0.26
Dextrose	2.00
$MgCl_2 \cdot 6H_2O$	0.15
KCl	0.07
NaCl	4.10
$NaC_2H_3O_2$	6.00

ductive life (40). Hemodialysis relieves or reduces many of the clinical characteristics of renal failure, but it has become increasingly recognized that this form of therapy is only a partial solution for treating uremia. In light of this, better artificial kidneys and hemodialysis programs must be developed.

CHAPTER 6

HIGH PRESSURE ANION-EXCHANGE CHROMATOGRAPHY

In order to monitor the removal of dialyzable, body-fluid constituents, a technique must be developed to separate and detect the variations in these component concentrations during the course of dialysis. An extensive review of body-fluid separation techniques revealed that the Oak Ridge National Laboratories (ORNL) have developed a method for separating body-fluid constituents in a forty-hour analysis period. This technique incorporates gradient elution, high pressure, ion-exchange chromatography. Investigators at the ORNL have successfully used ion-exchange chromatography in the separation and identification of carbohydrates (35, 36), naturally flourescing compounds (13, 45), and low molecular weight constituents (11, 12, 44, 48, 49, 59, 60, 61) in normal and pathological urine. Since many of the dialyzed constituents would be similar to urinary constituents, the chromatographic technique for separating urinary constituents was chosen as the analytical method for monitoring dialyzed components.

Figure 3 is a schematic of the high pressure, anion-exchange chromatographic system used in this project. This system consists of a two chamber gradient elution generator; a Lapp, Model LS-30, high pressure pump; a pressure indicator; a six-port sample injection valve; a jacketed, stainless steel, chromatographic column; a Chromatotronix, Model 230, dual wavelength, ultraviolet detector; a Linear

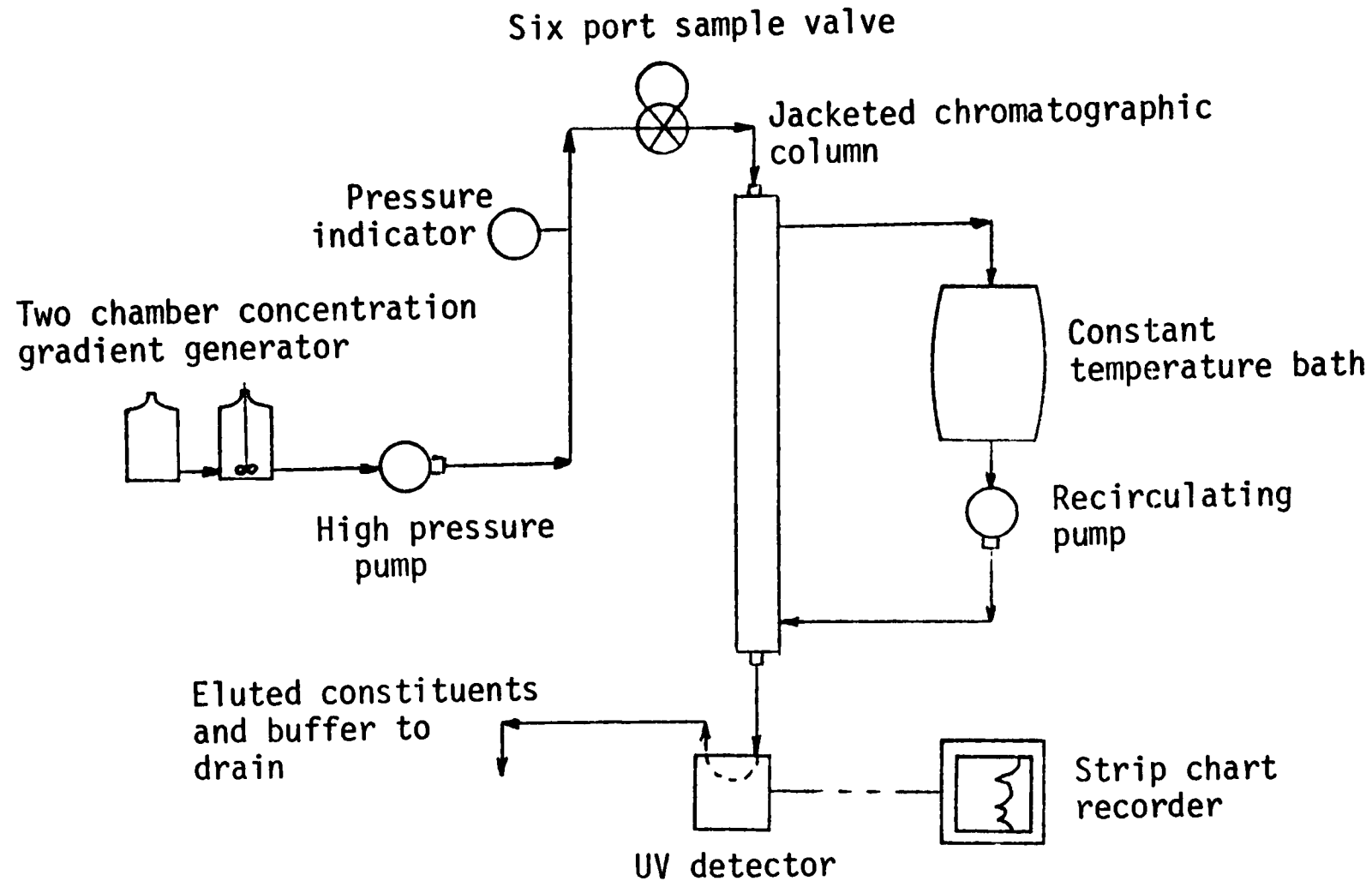

Figure 3. High pressure anion-exchange chromatographic system.

Instruments, dual pen-recorder; and a constant temperature recirculating bath. Table 2 shows the system's pertinent operating conditions and parameters. The ammonium acetate-acetic acid buffer is pumped to the chromatographic column by the high pressure pump. Five milliliters of the sample to be analyzed are introduced into the buffer stream by the sample injection valve. The eluted constituents from the chromatographic column then pass through the ultraviolet detector which monitors the light absorbance at 254 and 280 nm. The absorbance of each eluted constituent is then recorded on the strip chart recorder.

The resin used to separate the dialyzed, body fluid constituents was Bio Rad, Aminex A-27. This resin is classified as a strong anion-exchange, quarternary amine resin with an 8% cross linkage (14). The particle size of this resin ranges from 12 to 15 microns.

Figure 4 is a drawing of a typical chromatogram of the eluted constituents monitored in a dialysate sample. This chromatogram shows that forty-four dialyzed constituents in the dialysate sample can be separated and monitored. Since these constituents are in small concentrations, the change in absorbance or peak height will be directly proportional to the change in concentration.

Using this high pressure, anion-exchange chromatographic system, the change in concentration of forty-four dialyzed, body fluid constituents can be monitored during the course of dialysis. These data provide a critical check on the assumptions used in mathematically describing the removal of body-fluid solutes during hemodialysis.

TABLE 2

OPERATING CONDITIONS AND PARAMETERS FOR THE HIGH PRESSURE, ANION-EXCHANGE CHROMATOGRAPHIC SYSTEM

Condition or Parameter	Value
Column dimensions	0.94x150 cm
Resin	Bio Rad, A-27
Resin particle size	12-15 μ
Sample size	5 ml
Run time	48 hrs
Operating pressure	1400 psi
Eluent flow rate	80 ml/hr
Detector wave lengths	254 and 280 nm
Temperature program	Ambient, increasing to 60°C after 11 hr and 50 min
Eluent	Ammonium acetate-acetic acid buffer, pH 4.3, 0-6.0 mol/l
Gradient generator	Two chamber containing 3600 ml of de-ionized water and 3600 ml 6.0 mol/l buffer

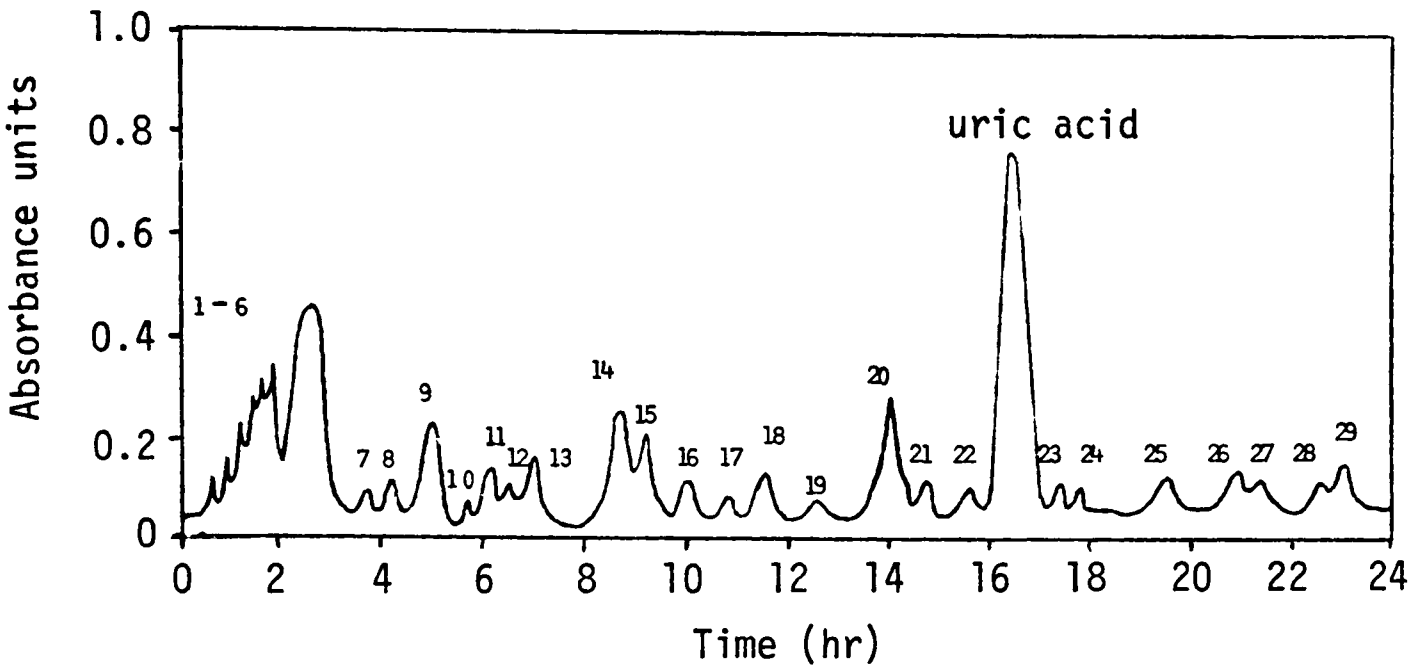

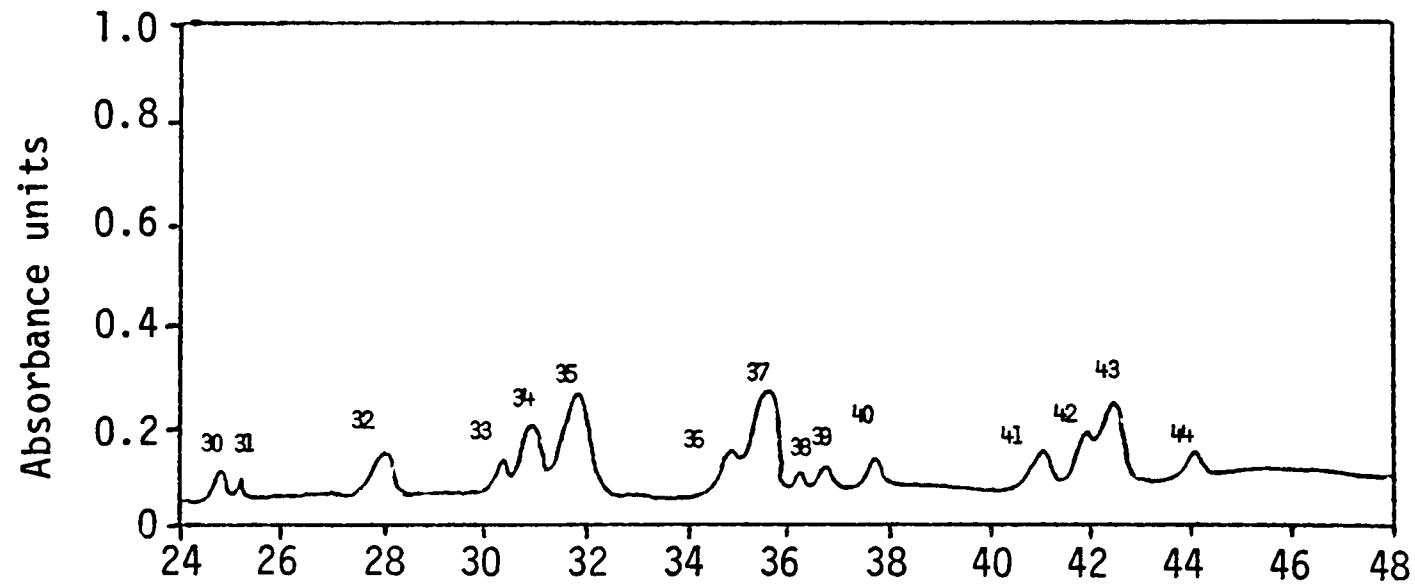

Figure 4. Illustration of a typical high pressure anion-exchange chromatogram.

CHAPTER 7

EXPERIMENTAL

Identification of Uremic Toxins

The initial experimental approach of this project was to isolate and identify uremic toxins which were slowly dialyzed through the CDAK membrane. In this approach, renal failure would be surgically or chemically induced in test animals. High pressure, anion-exchange chromatograms of the test animal, body-fluid constituents would be obtained before and after inducing renal failure. The variations in body-fluid constituents due to uremia would then be determined by comparing the anion-exchange chromatograms of normal and uremic body fluids. The abnormal constituents would then be collected and purified by vacuum evaporation to remove the ammonium acetate-acetic acid buffer. These purified components would then be identified by mass spectrophotometric analysis using a Varian MAT 711 mass spectrometer. Once these uremic constituents were identified, they could be monitored during hemodialysis to insure adequate hemodialysis therapy.

Although this was a sound experimental approach, it was found that there were many problems encountered in all the experimental phases. These problems included: (a) since this investigation delt with chronic uremia, experimental animals must be maintained on hemodialysis therapy for a significant length of time, (b) many of

the body-fluid samples were too dilute for sufficient chromatographic analysis, (c) purifying the eluted constituents was very time consuming and inexact, (d) the amounts of many eluted components were also not in sufficient quantity to obtain an adequate mass spectrophotometric analysis. Considering the length of time, money, and personnel required to solve these problems, a different approach was taken in this investigation.

Mathematical Model for Hemodialysis

To insure adequate and consistent hemodialysis therapy, a mathematical model could be developed to describe the mass transfer of dialyzable constituents during hemodialysis. This model could be used to predict the dialysis time required to remove a specified fraction of a dialyzable constituent in the body fluids at certain hemodialyzer operating conditions.

To develop and verify this predictive model, blood and dialysate samples were collected during the hemodialysis treatments of eight patients at the South Plains Dialysis Center. The artificial kidney used for each hemodialysis treatment was the Model 4, Cordis Dow Artificial Kidney (CDAK). During the sampling period, the blood and dialysate flow rates, the pressure drop across the CDAK, and the ultrafiltration pressure were recorded every fifteen minutes. The pressure drop across the CDAK was obtained by

$$(\Delta P)_{obs} = P_a - P_v \qquad (1)$$

where $(\Delta P)_{obs}$ = observed pressure drop across the CDAK

P_a = pressure at the arterial side of the CDAK

P_v = pressure at the venous side of the CDAK.

The ultrafiltration pressure was calculated by

$$P_{uf} = \frac{P_a + P_v}{2} + P' \qquad (2)$$

where P_{uf} = ultrafiltration pressure

P' = pressure in the dialysate side of the CDAK.

The values for the arterial and venous pressures and the pressure in the dialysate side of the CDAK were all obtained using a mercury manometer.

Procedures for Sample Collection and Chromatographic Analysis

The following procedure was used to collect blood samples for the hemodialysis treatments of six uremic patients:

1. Before sample collection, allow the blood and dialysate flow rates and ultrafiltration pressure to reach steady conditions (approximately twenty minutes after initiating hemodialysis).

2. At the beginning of the sampling period, record the blood and dialysate flow rates, the ultrafiltration pressure, the arterial and venous pressures, and simultaneously collect one milliliter arterial and venous blood samples.

3. For each sample, determine the blood hematocrit and the blood concentration of urea nitrogen and creatinine (the urea and creatinine blood concentrations were determined using Dow Diagnostests).

4. Record the blood and dialysate flow rates, the ultrafiltration pressure, and the arterial and venous pressures every fifteen minutes during the sampling interval.

5. At the end of the sampling period, simultaneously collect one milliliter arterial and venous blood samples and determine the hematocrit and the blood urea nitrogen and creatinine concentrations.

The data obtained from these samples were used to determine the model variables which affected the mass-transfer rates of urea and creatinine and to compare calculated and actual removal fractions of urea and creatinine.

The following procedure was used to collect dialysate samples for the hemodialysis treatments of two uremic patients and to analyze these samples by high pressure, anion-exchange chromatography:

1. Allow the blood and dialysate flow rates and the ultrafiltration pressure to reach steady conditions (approximately twenty minutes after initiating hemodialysis).

2. After steady conditions are achieved, collect five hundred milliliter dialysate samples at the dialysate outlet of the CDAK and record the blood and dialysate flow rates, the ultrafiltration pressure, and the arterial and venous pressures every fifteen minutes during the sampling interval.

3. At the end of the sampling interval, determine the urea nitrogen, creatinine, and uric acid concentrations in each dialysate sample using Dow Diagnostests.

4. Vacuum evaporate each dialysate sample at 0.0001 mm Hg and 30°C to dryness (approximately five hours per sample) using a Rinco Rotary Evaporator and a Model 15, Precision Vacuum Pump.

5. Store these dried samples in air tight, opaque containers at room temperature.

6. Immediately before injecting a dialysate sample into the high pressure, anion-exchange chromatograph, dissolve the sample in six milliliters of distilled and de-ionized water and separate the undissolved solids by centrifuging the sample for five minutes at 5000 RPM.

7. Inject five milliliters of the supernatent into the anion-exchange chromatograph.

8. Record the peak heights of each of the forty-four constituents eluted from the high pressure, anion-exchange chromatograph for each dialysate sample.

The data obtained from the chromatographic analysis of the dialysate samples were used to determine the change in concentration of the eluted constituents during the sampling period. This concentration-time data was then used to verify the development of the predictive model.

CHAPTER 8

MATHEMATICAL MODEL FOR HEMODIALYSIS

Mass Transfer Inside the CDAK

The artificial kidney used in this investigation was a Model 4, Cordis Dow Artificial Kidney (CDAK) shown in Figure 5. The CDAK is a continuous, countercurrent separation device utilizing both concentration and pressure driving forces across a semipermeable membrane to remove blood constituents. Table 3 lists the pertinent parameters for the CDAK. Blood flows inside the hollow fibers and dialysate flows on the outside of the fibers.

Figure 6 is a schematic of the mass flux of a blood solute, "i", out of a hollow fiber in the CDAK. In Figure 6, N_{iz} and N'_{iz} are the z-directional mass fluxes of "i" in the blood and dialysate. N_i, N_{im}, and N'_i are the r-directional mass fluxes of "i" through the blood, membrane, and dialysate. Assuming that there are no extra-dialysis sources or sinks of the dialyzed solutes, the steady-state mass balance for n dialyzable constituents is

$$\nabla \cdot N_j = 0 \qquad (3)$$

where j = 1,2,3,.....,n.

Since there are hundreds of constituents in the blood, the generalized relations for the mass flux of each dialyzed solute quickly become impractical to use. However, if the dialyzed constituents in the blood

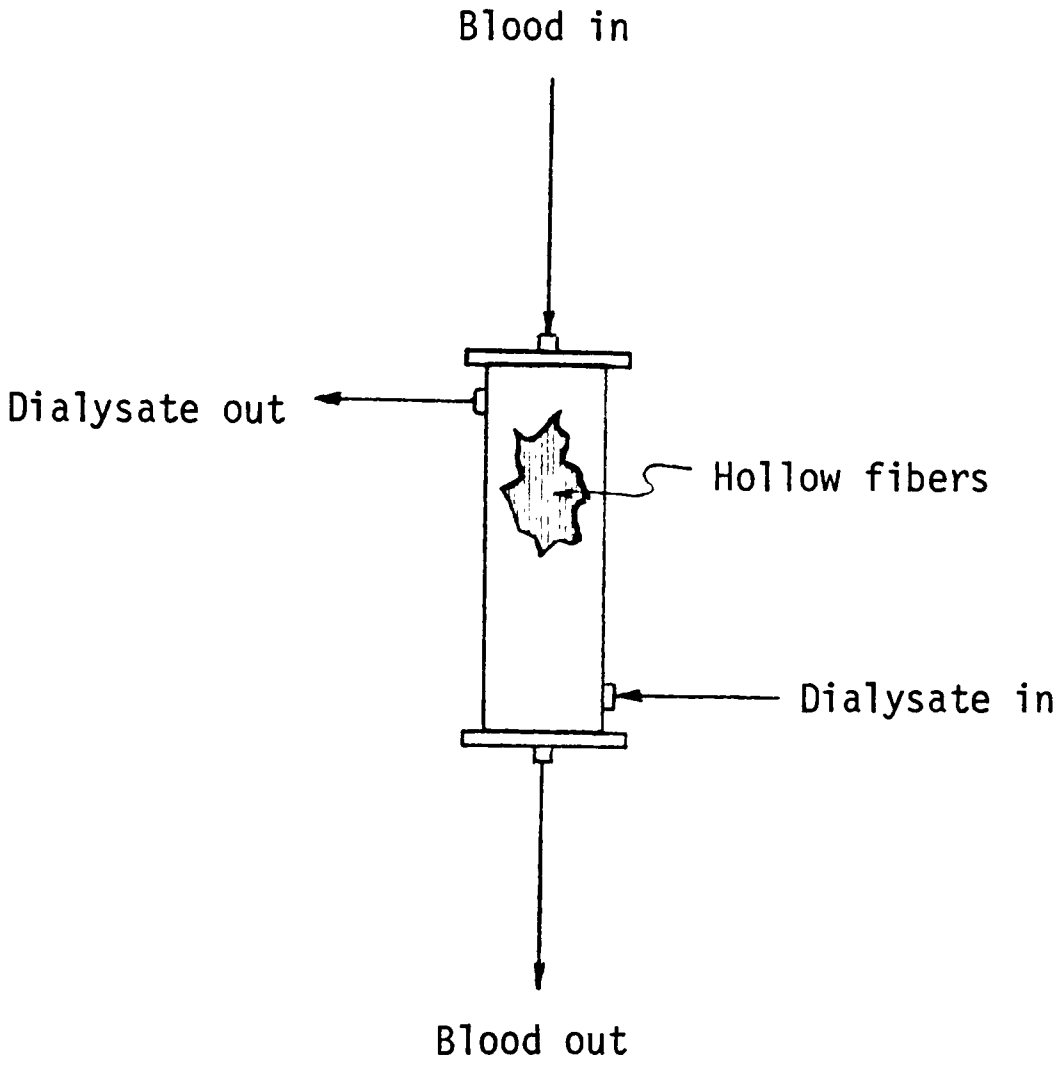

Figure 5. Schematic of the Model 4 Cordis Dow Artificial Kidney (CDAK).

TABLE 3

MODEL 4 CORDIS DOW ARTIFICIAL KIDNEY PARAMETERS

Parameter	Value
Blood volume	100 ml
Dialysate volume	100 ml
Fiber material	Regenerated cellulose
Number of fibers	13,500
Fiber length	16 cm
Fiber inside diameter	200 μ
Fiber wall thickness	30 μ
Mass transfer area	1.3 sq m

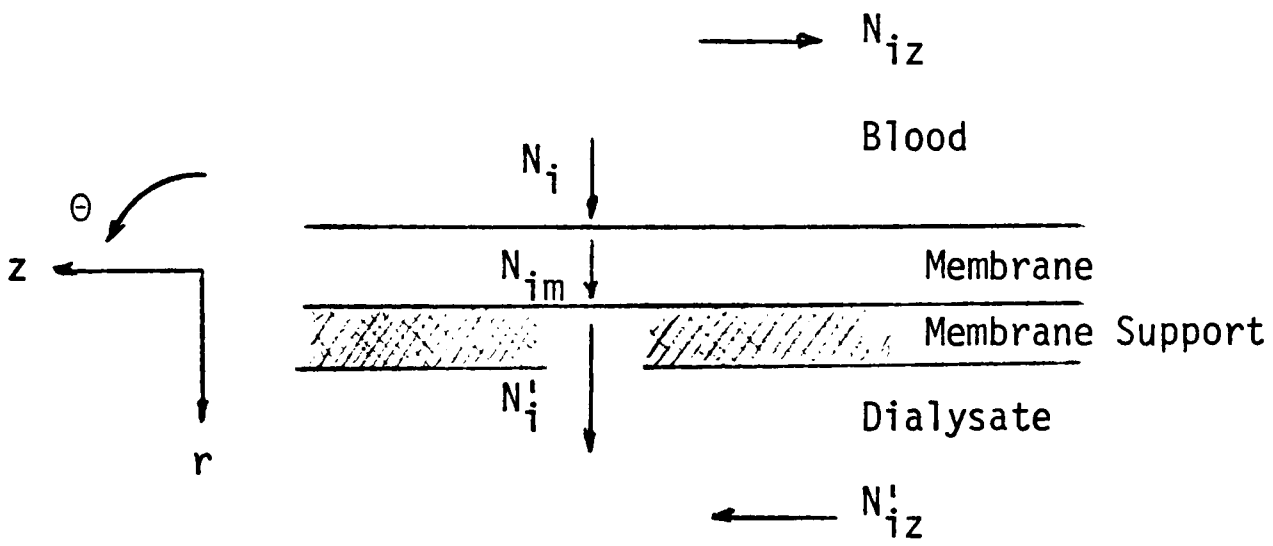

Figure 6. Mass flux of a dialyzable constituent from a hollow fiber in the CDAK.

are in small concentrations, the mass flux of each solute can be approximated by a binary, steady-state relation. This binary, steady-state approximation has been previously used in the development of hemodialysis models (4, 5, 52, 54, 55).

Assuming that blood can be treated as a homogeneous fluid with constant density and viscosity (54), the r-directional mass flux of a solute through the blood can be expressed as

$$N_i = -\mathcal{D}_{iB} \frac{\partial C_i}{\partial r} + x_i(N_i + N_B) \qquad (4)$$

where N_i = r-directional mass flux of "i" in the blood

$\mathcal{D}_{iB}$ = diffusivity of "i" in the blood

C_i = concentration of "i" in the blood

x_i = mass fraction of "i" in the blood moving in the r-direction

N_B = r-directional mass flux of the blood.

Since water makes up the majority of the blood phase constituents (4, 54), the mass flux of a dialyzed solute can be further approximated by

$$N_i = -\mathcal{D}_{iB} \frac{\partial C_i}{\partial r} + x_i(N_i + N_w) \qquad (5)$$

where N_w = r-directional mass flux of water.

In order to simplify the mass flux of "i" due to bulk flow, it is necessary to make two assumptions: (a) the r-directional mass flux of water is much greater than the r-directional mass flux of "i"

and (b) a constant fraction of "i" in the blood phase is transmitted to the blood-membrane interface by bulk flow in the r-direction. These two assumptions have been previously used by Babb, et al. (4) and by Ramierz, et al. (54) in their developments of a hemodialysis model. By combining these assumptions, the bulk flow term in equation (5) can be approximated by

$$x_i(N_i + N_w) = \Psi_i \, \overline{C}_i \, v_w \tag{6}$$

where Ψ_i = fraction of "i" in the blood phase transmitted to the blood-membrane interface by bulk flow in the r-direction

$\overline{C}_i$ = integral average bulk concentration of "i" in the blood

v_w = r-directional velocity of water.

Combining equations (5) and (6) and assuming that the mass flux of "i" due to diffusion occurs only in the r-direction (4, 5, 52, 54, 55) yields

$$N_i = -\mathcal{D}_{iB} \frac{dC_i}{dr} + \Psi_i \, \overline{C}_i \, v_w. \tag{7}$$

Assuming that the major blood-side resistance for the r-directional mass flux of "i" occurs across a thin, stagnant film, the r-directional mass flux of "i" in the blood and the r-directional velocity of water can be expressed by

$$N_i = (N_i)_{r_o} \left(\frac{r_o}{r}\right) \tag{8}$$

and

$$v_w = (v_w)_{r_o}\left(\frac{r_o}{r}\right) \tag{9}$$

where $(N_i)_{r_o}$ = r-directional mass flux of "i" at r_o

$(v_w)_{r_o}$ = r-directional velocity of water at r_o

r_o = distance from the center of the fiber to the stagnant blood film.

These mass fluxes through the blood and dialysate films and through the membrane are illustrated in Figure 7. Substituting equations (8) and (9) into equation (7) yields

$$(N_i)_{r_o}\left(\frac{r_o}{r}\right) = -\mathcal{D}_{iB}\frac{dC_i}{dr} + \Psi_i\,\overline{C}_i(v_w)_{r_o}\left(\frac{r_o}{r}\right) \tag{10}$$

For a constant diffusivity, equation (10) can be integrated from r_o to r_1 and from $\overline{C}_i$ to C_{im}. This integration yields

$$(N_i)_{r_o} = \left[\frac{\mathcal{D}_{iB}}{r_o \ell n\left(\frac{r_1}{r_o}\right)}\right](\overline{C}_i - C_{im}) + \Psi_i\,\overline{C}_i(v_w)_{r_o} \tag{11}$$

where r_1 = distance from the center of the fiber to the blood-membrane interface

C_{im} = concentration of "i" in the blood at the blood-membrane interface.

Assuming that the thickness of the stagnant film is much less than r_o, then

$$\delta_f \cong r_o\,\ell n\left(\frac{r_1}{r_o}\right). \tag{12}$$

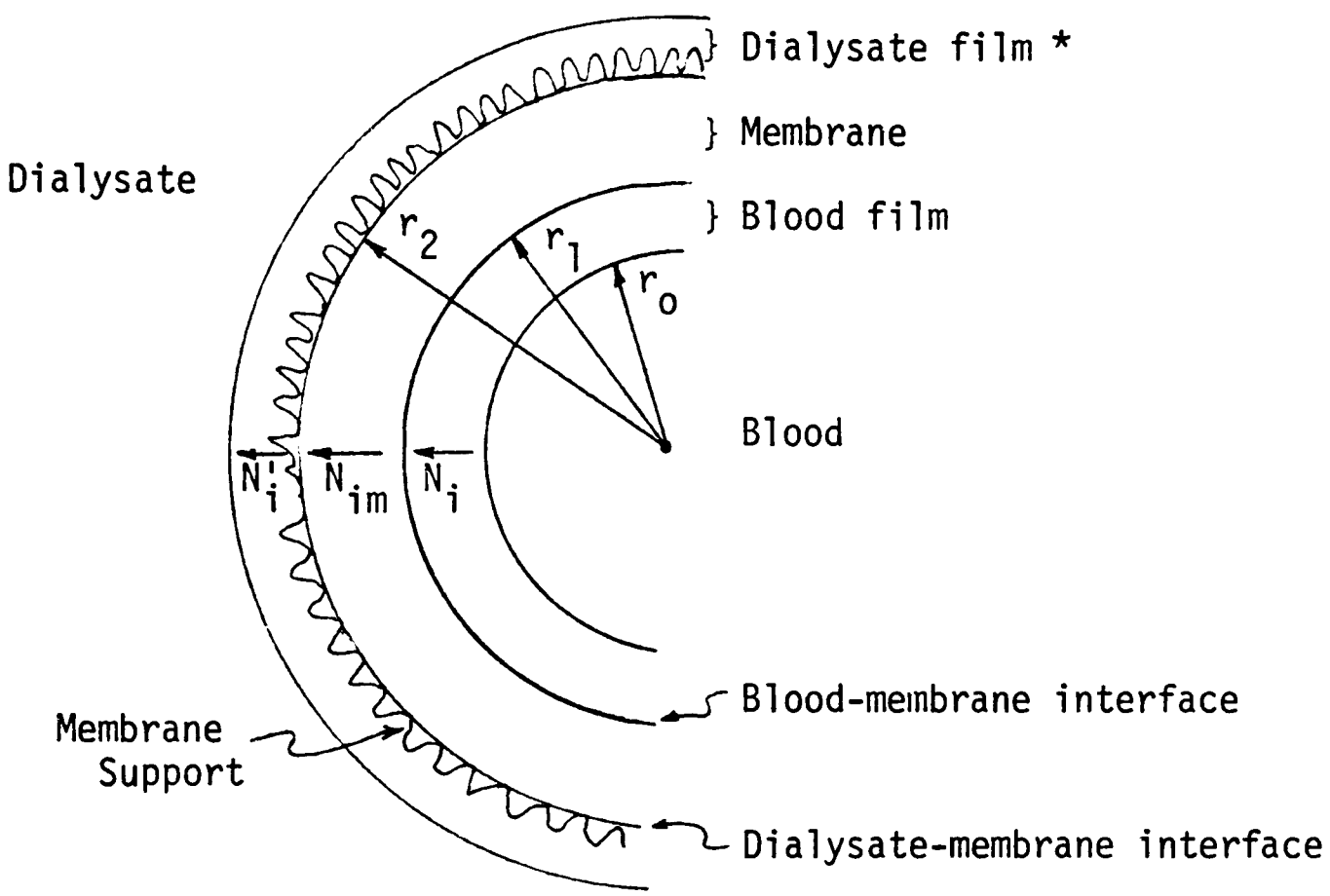

*The dialysate film includes the fluid in the membrane support.

Figure 7. Mass flux of "i" through the stagnant blood and dialysate films and through the membrane.

Substituting equation (12) into equation (11) yields

$$(N_i)_{r_o} = k_i (\overline{C}_i - C_{im}) + \Psi_i \overline{C}_i (v_w)_{r_o} \qquad (13)$$

where $k_i = \frac{\mathcal{D}_{iB}}{\delta_f}$ = local mass-transfer coefficient for "i" across the stagnant blood film

δ_f = thickness of the stagnant blood film.

By using similar approximations incorporated in developing equation (13), the r-directional mass flux through the dialysate film is

$$(N_i')_{r_2} = k_i' (C_{im}' - \overline{C}_i') + \Psi_i' \overline{C}_{im} (v_w)_{r_2} \qquad (14)$$

where $(N_i')_{r_2}$ = r-directional mass flux of "i" at r_2

k_i' = local mass-transfer coefficient for "i" across the stagnant dialysate film and membrane support

C_{im}' = concentration of "i" in the dialysate at the dialysate-membrane interface

Ψ_i' = fraction of "i" in the dialysate at the dialysate-membrane interface transmitted to the bulk dialysate by bulk flow in the r-direction

$\overline{C}_i'$ = integral average bulk phase concentration of "i" in the dialysate

$(v_w)_{r_2}$ = r-directional velocity of water at r_2

r_2 = distance from the center of the fiber to the dialysate-membrane interface.

Incorporating similar approximations used in developing equations (13) and (14) and since the membrane thickness is small compared to r_1 (17), the mass flux of "i" through the membrane can be expressed as

$$(N_{im})_{r_1} = k_{im}[(C_{im})_B - (C_{im})_D] + \Psi_{im}(C_{im})_B (v_w)_{r_1} \qquad (15)$$

where $(N_{im})_{r_1}$ = r-directional mass flux of "i" at r_1

k_{im} = local mass-transfer coefficient for "i" in the membrane

$(C_{im})_B$ = concentration of "i" on the blood-side membrane surface

$(C_{im})_D$ = concentration of "i" on the dialysate-side membrane surface

Ψ_{im} = fraction of "i" on the blood-side membrane surface transmitted through the membrane by bulk flow

$(v_w)_{r_1}$ = r-directional velocity of water at r_1.

Equation (15) can be expressed in terms of a membrane permeability by incorporating an equilibrium coefficent relating the fluid-membrane interface concentrations to the membrane surface concentrations. Using this equilibrium coefficient, equation (15) can be expressed as

$$(N_{im})_{r_1} = P_{im}\,(C_{im} - C'_{im}) + \Psi_{im}\Gamma_{im}C_{im}(v_w)_{r_1} \qquad (16a)$$

where $P_{im} = k_{im}\,\Gamma_{im}$ (16b)

$$\Gamma_{im} = C_{im}/(C_{im})_B = (C_{im})_D/C'_{im} \qquad (16c)$$

P_{im} = permeability of "i" in the membrane

Γ_{im} = equilibrium coefficient relating the blood- and dialysate-membrane interface concentrations of "i" to the membrane surface concentrations of "i".

Equation (16a) assumes that the equilibrium coefficient is the same for both sides of the membrane. This assumption has also been used by Ramirez, et al. (54). At a steady state, the mass flux of "i" at any point along the membrane can be expressed by

$$\overline{N}_i = (N_i)_{r_o}\left(\frac{r_o}{r_1}\right) = (N_{im})_{r_1} = (N'_i)_{r_2}\left(\frac{r_2}{r_1}\right) \qquad (17)$$

where $\bar{N}_i$ = r-directional mass flux of "i" at r_1.

Combining equations (13), (14), (16a) and (17) yields

$$\bar{N}_i = K_i(\bar{C}_i - \bar{C}'_i) + K_i\left(\frac{\Psi_i (v_w)_{r_o} \bar{C}_i}{k_i} + \frac{\Psi_{im}\Gamma_{im}(v_w)_{r_1} C_{im}}{P_{im}} + \frac{\Psi'_i (v_w)_{r_2} C'_{im}}{k'_i}\right) \quad (18)$$

(Diffusion) (Bulk Flow)

where $\frac{1}{K_i} = \left(\frac{r_o}{k_i r_1} + \frac{1}{P_{im}} + \frac{r_2}{k'_i r_1}\right)$

K_i = local overall mass-transfer coefficient for "i" at any point along the membrane.

In order to express the bulk flow term in equation (18) in terms of the bulk blood concentration of "i", it is necessary to approximate relationships between $\bar{C}_i$ and C_{im}, and between $(C_{im})_B$ and $(C_{im})_D$. These relationships are defined as

$$\beta_i = (C_{im})/(\bar{C}_i) \quad ; \quad 0 \leq \beta_i \leq 1 \quad (19a)$$

and

$$\beta_{im} = (C_{im})_D/(C_{im})_B \quad ; \quad 0 \leq \beta_{im} \leq 1 \quad (19b)$$

where β_i = a constant relating the concentration of "i" in the blood at the blood-membrane interface to the bulk phase blood concentration of "i"

β_{im} = a constant relating the membrane surface concentrations of "i".

Using these constants, it is assumed (a) that the bulk dialysate concentration of "i" is much less than the bulk blood concentration of "i", (b) that a constant fraction of "i" in the blood phase is transfered to the blood-membrane interface, (c) that a constant fraction of "i" on the blood-side membrane surface is transfered

through the membrane, and (d) that the mass flux of "i" is slow. Combining equations (16c), (18), (19a), and (19b), the final expression for the mass flux of "i" at any point along the membrane is

$$\overline{N}_i = K_i (\overline{C}_i - C_i') + K_i \overline{v}_w \phi_i \overline{C}_i \qquad (20)$$

where $\overline{v}_w = (v_w)_{r_o}(\frac{r_o}{r_1}) = (v_w)_{r_1} = (v_w)_{r_2}(\frac{r_2}{r_1})$

$$\phi_i = [\frac{\Psi_i r_o}{k_i r_1} + \frac{\Psi_{im}\Gamma_{im}\beta_i}{P_{im}} + \frac{\Psi_i \Gamma_{im}^2 \beta_{im}\beta_i r_2}{k_i' r_1}]$$

$\overline{v}_w\phi_i$ = local overall ultrafiltration coefficient.

Equation (20) shows that the mass flux due to ultrafiltration, $K_i\overline{v}_w\phi_i\overline{C}_i$, and the mass flux due to diffusion, $A_iK_i(\overline{C}_i - \overline{C}_i')$, can be separated into two separate terms in the overall expression for the mass-transfer rate of a dialyzable constituent at any point along the artificial kidney membrane.

Predictive Model for Hemodialysis

The schematic of the hemodialysis system to be modeled is shown in Figure 8. This system treats the body-fluid pools as a single, well-mixed pool with a constant volume (V). The outlet blood concentration of "i", $\langle C_i \rangle_2$, is the integral average concentration of a solute immediately after exiting the artificial kidney. This concentration also remains constant in the tubing from the aftificial kidney to the body-fluid pool. The inlet blood concentration of "i", $\langle C_i \rangle_1$, is assumed to be at the same concentration

$$\langle C_i \rangle_2 = \frac{\int_o^R C_i dr}{\int_o^R dr}$$

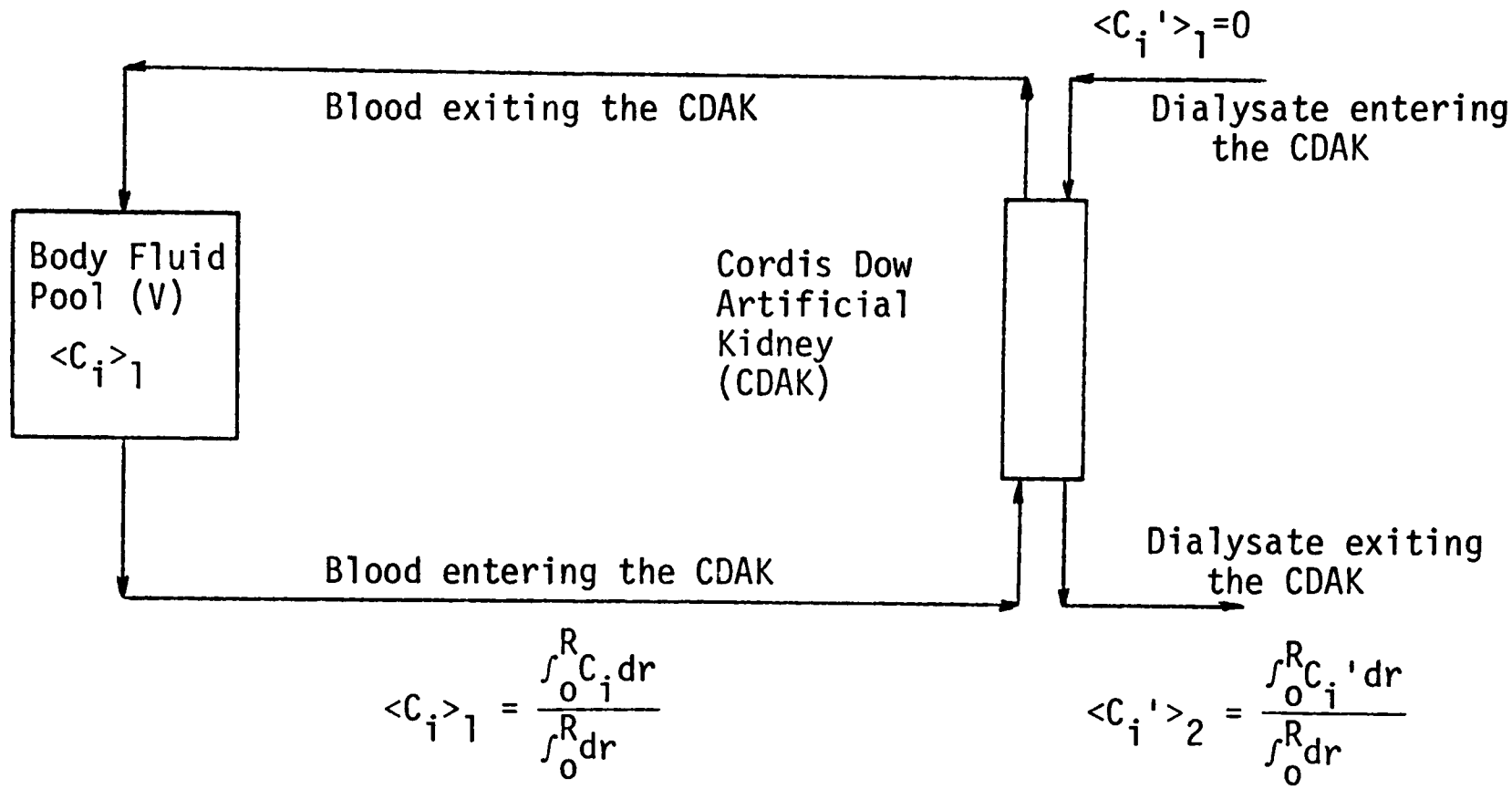

Figure 8. Schematic of the model hemodialysis system.

in the body-fluid pool, and this concentration is assumed not to vary in the tubing from the body-fluid pool to the artificial kidney. The outlet dialysate concentration of "i", $\langle C_i' \rangle_2$, does not vary in the tubing leaving the kidney, and since the dialysate flow is single pass, the inlet dialysate concentration of "i", $\langle C_i' \rangle_1$, is zero. It is also assumed that since the volume of the body-fluid pool is much greater than the volume inside the tubing and the artificial kidney, the change in solute concentration in the pool during dialysis is much less than the change in solute concentration in the aftificial kidney and that there is no accumulation of "i" in the CDAK.

Using these assumptions, the total steady-state mass-transfer rate of "i" per pass through the CDAK at any time during dialysis can be expressed by

$$\dot{m}_{iT} = Q_B[\langle C_i \rangle_1 - \langle C_i \rangle_2] = Q_D \langle C_i' \rangle_2 \tag{21}$$

$$\dot{m}_{iT} = -V \frac{d(\langle C_i \rangle_1)}{dt} \tag{22}$$

$$\dot{m}_{iT} = D_{iT} \langle C_i \rangle_1 \tag{23}$$

where $\dot{m}_{iT}$ = total mass-transfer rate of "i" per pass through the CDAK at any time during hemodialysis

Q_B = blood flow rate

Q_D = dialysate flow rate

$\langle C_i \rangle_1$ = integral average inlet blood concentration of "i"

$\langle C_i \rangle_2$ = integral average outlet blood concentration of "i"

$\langle C_i' \rangle_2$ = integral average outlet dialysate concentration of "i"

V = body fluid volume

t = dialysis time

D_{iT} = total dialysance of "i".

Equation (21) is a steady-state material balance around the CDAK. Equation (22) is the expression for the removal of a solute from a well-mixed, constant volume compartment. Equation (23) incorporates the term dialysance. This term was first introduced by Wolf (68) and is defined as the volumetric flow rate of blood that is completely cleared of a solute per pass through the artificial kidney. The dialysance of a solute can also be expressed in common mass-transfer terms. To develop this expression, equation (20) needs to be integrated to give an expression for the total mass-transfer rate of "i" per pass through the CDAK. For a constant overall mass-transfer coefficient, ϕ_i, $\bar{v}_w$, and total mass-transfer area, the result of this integration is

$$\dot{m}_{iT} = A_T K_{iT} [\Delta \langle \bar{\bar{C}}_i \rangle_{lm}] \tag{24}$$

where

$$\Delta \langle \bar{\bar{C}}_i \rangle_{lm} = \left\{ \frac{\langle \bar{\bar{C}}_i \rangle_1 - \langle \bar{\bar{C}}_i \rangle_2 - \langle C_i' \rangle_2}{\ell n \left[\frac{\langle \bar{\bar{C}}_i \rangle_1 - \langle \bar{\bar{C}}_i' \rangle_2}{\langle \bar{\bar{C}}_i \rangle_2} \right]} \right\}$$

$$\langle \bar{\bar{C}}_i \rangle_1 = (1 + \phi_i \bar{v}_w) \langle C_i \rangle_1$$

$$\langle \bar{\bar{C}}_i \rangle_2 = (1 + \phi_i \bar{v}_w) \langle C_i \rangle_2$$

A_T = total mass-transfer area in the CDAK with respect

to the inside diameter of the fibers

K_{iT} = overall mass transfer coefficient for "i" in the CDAK

$\Delta\langle\bar{\bar{C}}_i\rangle_{lm}$ = effective logarithemic-mean concentration driving force in the CDAK

$\langle\bar{\bar{C}}_i\rangle_1$ = effective blood concentration of "i" entering the CDAK

$\langle\bar{\bar{C}}_i\rangle_2$ = effective blood concentration of "i" exiting the CDAK.

The effective blood concentrations in equation (24) are defined to include the mass transfer due to ultrafiltration and the diffusive mass transfer. Combining equations (23) and (24), the expression for the dialysance of "i" is

$$D_{iT} = \frac{A_T K_{iT}[\Delta\langle\bar{\bar{C}}_i\rangle_{lm}]}{\langle C_i\rangle_1} . \qquad (25)$$

The development of equation (20) can also be used to justify the separation of the diffusive and ultrafiltrative mass-transfer rates in terms of dialysances. This expression is shown by

$$\dot{m}_{iT} = D_{id}\langle C_i\rangle_1 + D_{iuf}\langle C_i\rangle_1 \qquad (26)$$

where D_{id} = dialysance of "i" due to diffusion

D_{iuf} = dialysance of "i" due to ultrafiltration.

Assuming that the blood and dialysate flow rates, the membrane properties, the ultrafiltration pressure, and the diffusive and ultrafiltrative dialysances of "i" remain constant (55), equations (22) and (26) can be combined and integrated to yield

$$E_i = 1 - \exp\left[-\frac{\eta_i D_{id}\, t}{V}\right] \qquad (27)$$

where $\eta_1 = 1 + \frac{D_{iuf}}{D_{id}}$ = ultrafiltration correction factor

E_i = fraction of "i" in the body fluid removed during dialysis

t = dialysis time.

Equation (27) is a model for the hemodiaylsis system shown in Figure 7; however, in actual hemodialysis, there is a possibility of a reduction in mass-transfer area probably due to total or partial fiber occlusion (30). From equation (25), the dialysance of a solute is directly proportional to the area available for mass transfer; therefore, a mass-transfer area correction factor on the dialysance term could account for the possible decrease in mass-transfer area. At a constant volumetric blood flow rate, the decrease in mass-transfer area would also be equal to the decrease in flow area which would be indicated by an increase in pressure drop across the artificial kidney. Using these relationships, an area correction factor may be defined as

$$\alpha = \frac{(\Delta P)_{calc}}{(\Delta P)_{obs}} \quad ; \quad 0 \leq \alpha \leq 1 \qquad (28)$$

where α = area correction factor or the fraction of the CDAK mass transfer area available for mass transfer

$(\Delta P)_{calc}$ = pressure drop across the CDAK calculated from equation (A3) in Appendix I and is a function of blood flow and hematocrit

$(\Delta P)_{obs}$ = pressure drop across the CDAK observed during hemodialysis.

Combining the mass-transfer area correction factor with equation (27) yields the final predictive model,

$$E_i = 1 - \exp\left[-\frac{\alpha \eta_i D_{id} t}{V}\right]. \qquad (29)$$

In order to use equation (29), the solute ultrafiltration correction factor, the solute diffusive dialysance, the pressure drop across the aftificial kidney, the patient's hematocrit, the blood flow rate, and the body fluid volume must be known. Once these values are obtained, equation (29) will predict the dialysis time and hemodialyzer operating conditions required to remove a specified fraction of a dialyzable constituent from the body fluids.

CHAPTER 9

RESULTS AND DISCUSSION

Eight patients undergoing hemodialysis therapy at the South Plains Dialysis Center were used as experimental subjects in this investigation. Model 4, Cordis Dow Artificial Kidneys (CDAK) were used in all the hemodialysis treatments. Three hemodialysis treatments of two uremic patients were used to evaluate the change in concentration of forty-seven dialyzed constituents every fifteen minutes during hemodialysis. These concentration-time data were then used to verify the development of the predictive model. The data obtained from the hemodialysis treatments of six uremic patients were used to evaluate the effect of mass-transfer area and ultrafiltration on the mass-transfer rate of urea and creatinine. These data were also used to compare removal fractions of urea and creatinine calculated from the predictive model to the actual observed removal fractions.

Verification of Model Development

The changes in the dialysate concentration of forty-seven dialyzed constituents every fifteen minutes during the sampling interval were obtained from three hemodialysis treatments of two uremic patients. The hemodialysis conditions for these treatments are listed in Table 4.

To verify the model development from this concentration-time data, equations (21), (22) and (23) can be combined to yield the

TABLE 4

OPERATING CONDITIONS FOR THE DIALYSIS TREATMENTS USED TO MONITOR THE DIALYSATE CONCENTRATION OF DIALYZED CONSTITUENTS

Condition	Treatment Number 1*	2**	3**
Ultrafiltration pressure (mm Hg)	100	200	400
Pressure drop across the CDAK (mm Hg)	20	15	17
Blood flow rate (ml/min)	200	200	200
Dialysate flow rate (ml/min)	500	500	500

* Dialysis treatment for patient JP
** Dialysis treatment for patient AC

expected relationship between the change in the dialysate concentration with respect to dialysis time for dialyzable constituents. This relationship is shown by

$$\sigma_i = -\frac{D_{iT}}{V} = \frac{d[\ell n \langle C_i' \rangle_2]}{dt} \qquad (30)$$

where $\langle C_i' \rangle_2$ = integral average of the dialysate concentration of "i" exiting the CDAK (mg %)

t = dialysis time (hr)

D_{iT} = total dialysance of "i" (ml/hr)

V = total body fluid volume (ml)

σ_i = ratio of D_i to V (hr^{-1}).

In the development of the predictive model, the dialysance of a solute and the body fluid volume were assumed to remain constant during the dialysis period; therefore, the ratio of the solute dialysance to the body fluid volume, σ_i, should also remain constant. This indicates that the relationship between $\ell n \langle C_i' \rangle_2$ and dialysis time should be linear. Figures 9 and 10 are two typical examples of the $\ell n \langle C_i' \rangle_2$ versus time plots of the monitored constituents during the sampling interval. These figures illustrate that a linear relationship existed between $\ell n \langle C_i' \rangle_2$ and time and that the values for σ_i were constant for each monitored constituent. Values for σ_i and a correlation coefficient, R_i, for each monitored constituent were calculated from the slope of a regression analysis of $\ell n \langle C_i' \rangle_2$ versus time. These calculated values for σ_i and R_i are tabulated in Table 5. The correlation coefficient for the fifteen data points

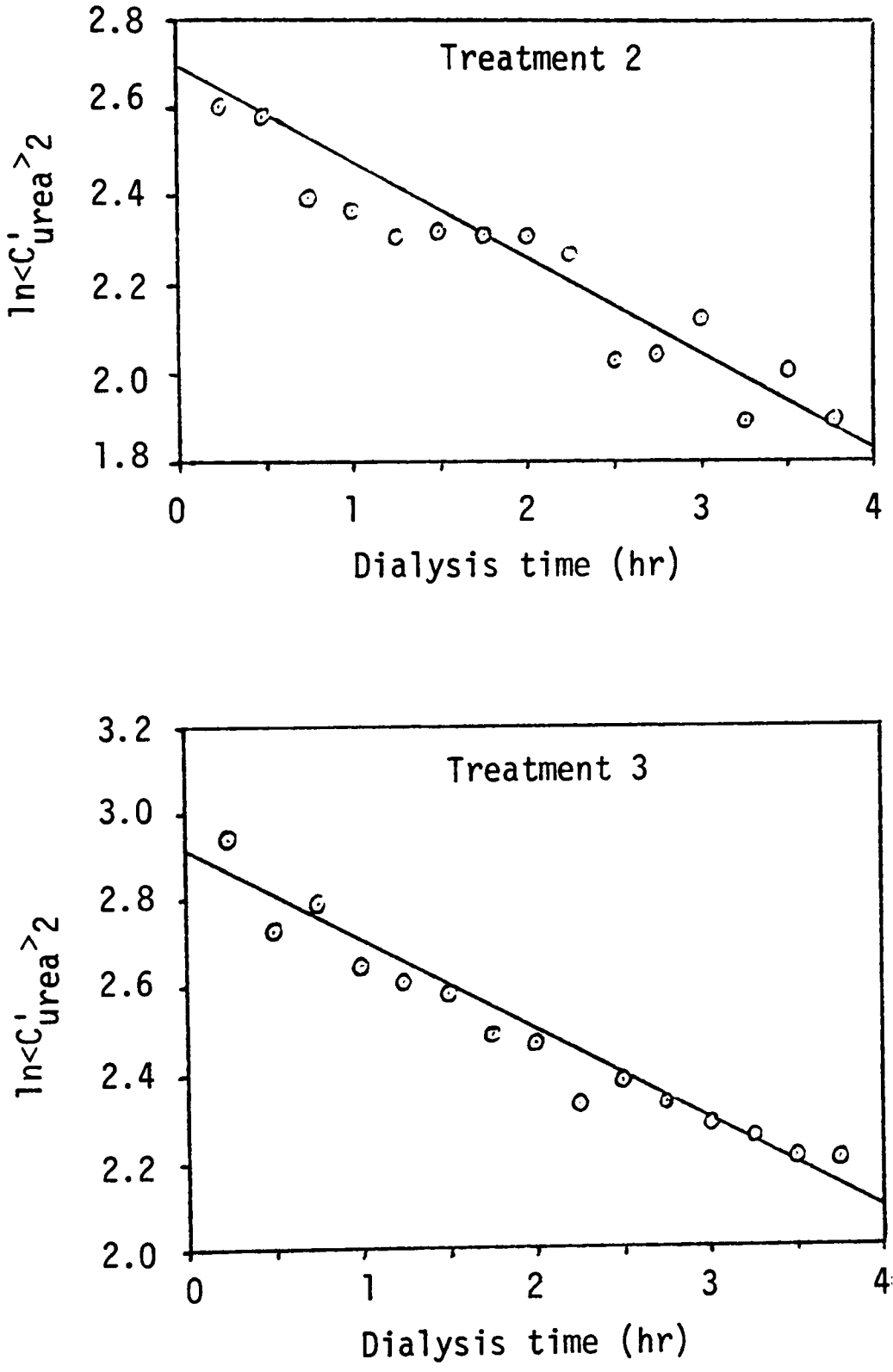

Figure 9. Urea concentration-time relationships for hemodialysis treatments 2 and 3.

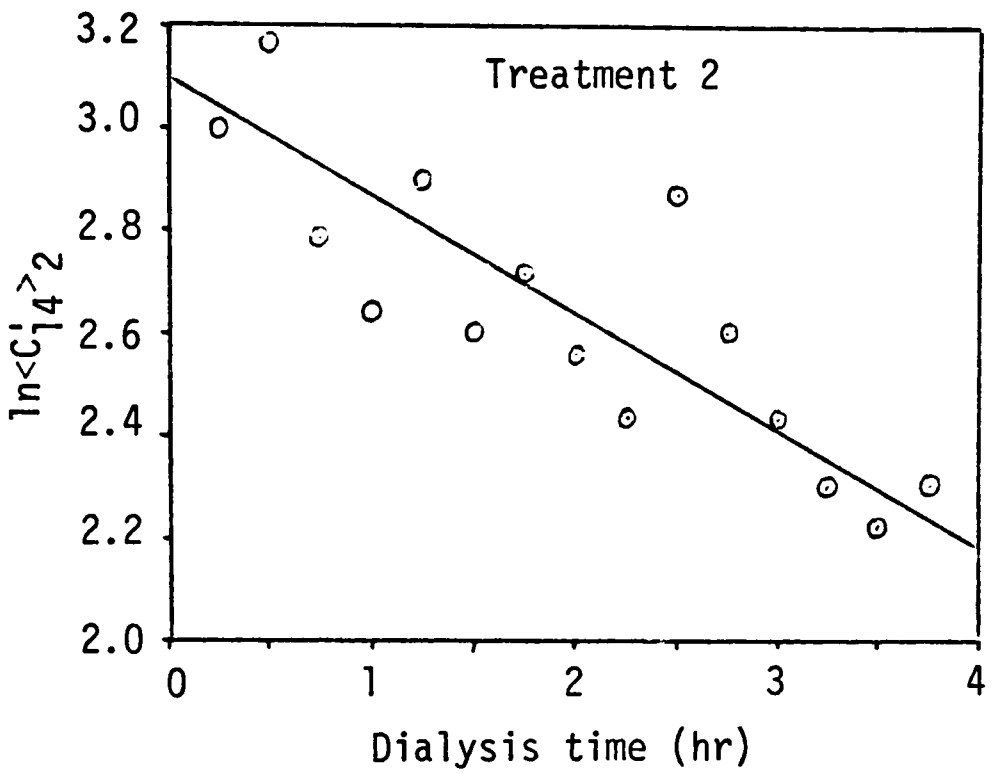

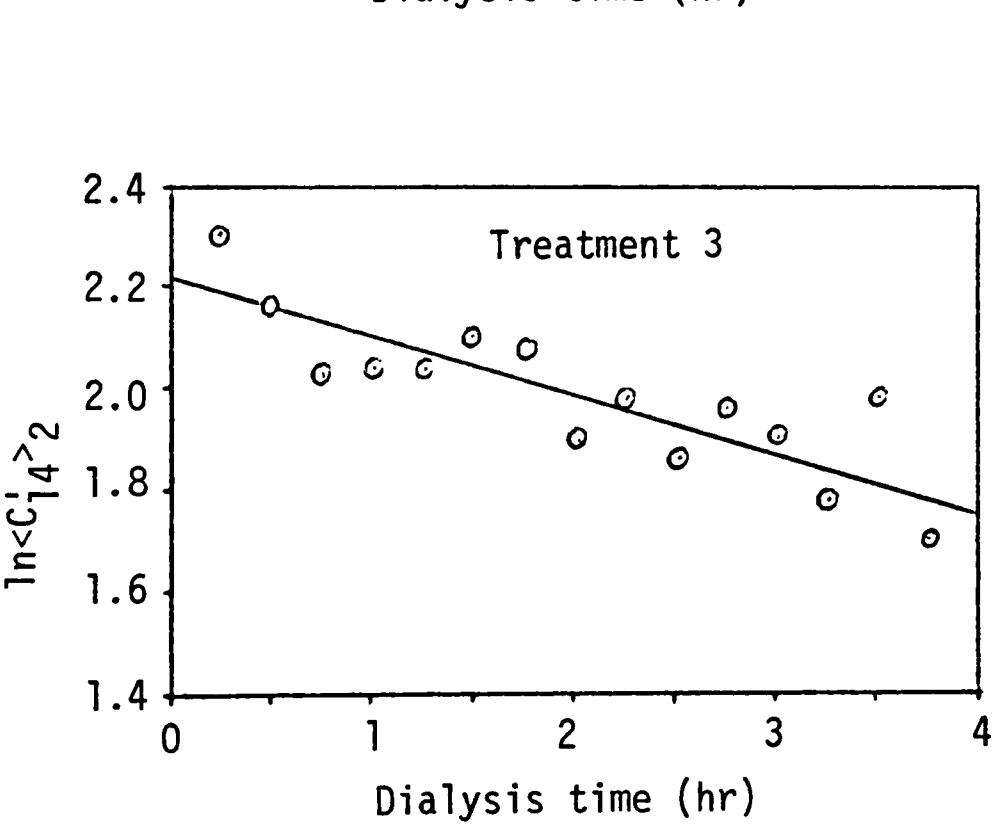

Figure 10. Peak number 14 concentration-time relationships for hemodialysis treatments 2 and 3.

TABLE 5

THE RELATIONSHIP BETWEEN THE DIALYSATE CONCENTRATION OF MONITORED CONSTITUENTS DURING DIALYSIS

Components Monitored by Dow Diagnostests	Treatment 1		Treatment 2		Treatment 3	
	σ_i hr^{-1}	R_i	σ_i hr^{-1}	R_i	σ_i hr^{-1}	R_i
Urea	0.190	0.97	0.221	0.95	0.209	0.97
Creatinine	0.155	0.60	0.187	0.92	0.175	0.67
Uric Acid	0.143 0.138*	0.74 0.70	0.148 0.152*	0.60 0.64	0.137 0.141*	0.71 0.58
Peak Numbers of Unknown Components Monitored by Chromatography						
1	0.249	0.84	0.211	0.92	0.180	0.91
2	0.200	0.81	0.233	0.98	0.165	0.92
3	0.186	0.71	0.225	0.98	0.165	0.85
4	0.217	0.74	0.232	0.97	0.174	0.90
5	0.174	0.60	0.238	0.95	0.172	0.89
6	0.176	0.60	0.235	0.96	0.168	0.88
7	0.143	0.75	0.201	0.70	0.142	0.80
8	0.140	0.63	0.126	0.70	0.084	0.90
9	---	--	0.190	0.86	0.192	0.86
10	0.115	0.54	0.224	0.95	0.222	0.55

TABLE 5 (Continued)

11	0.138	0.70	0.154	0.89	0.153	0.91
12	---	--	0.143	0.75	0.137	0.92
13	0.176	0.58	0.143	0.71	0.122	0.82
14	0.085	0.52	0.230	0.60	0.118	0.88
15	0.100	0.52	0.267	0.87	0.294	0.82
16	0.090	0.54	0.124	0.92	0.126	0.57
17	0.203	0.55	0.457	0.92	0.315	0.96
18	0.296	0.68	0.265	0.71	0.207	0.52
19	0.291	0.68	0.176	0.57	0.148	0.66
20	0.205	0.69	0.156	0.53	0.168	0.99
21	0.252	0.75	0.208	0.61	0.234	0.81
22	0.219	0.78	0.230	0.60	0.192	0.86
23	0.292	0.82	0.235	0.52	0.177	0.81
24	---	--	0.337	0.64	0.211	0.87
25	0.292	0.82	0.251	0.73	0.236	0.85
26	0.183	0.88	0.180	0.82	0.192	0.52
27	0.100	0.52	0.400	0.85	0.336	0.82
28	0.110	0.53	0.232	0.79	0.221	0.53
29	0.213	0.67	0.308	0.70	0.254	0.84
30	0.228	0.75	0.228	0.73	0.241	0.93
31	---	--	0.258	0.84	0.267	0.89
32	0.276	0.95	0.253	0.57	0.220	0.94
33	0.262	0.91	0.207	0.59	0.215	0.83

TABLE 5 (Continued)

34	0.220	0.87	0.092	0.52	0.092	0.56
35	0.263	0.92	0.168	0.77	0.184	0.92
36	---	--	0.124	0.57	0.232	0.93
37	0.178	0.87	0.248	0.56	0.263	0.83
38	0.227	0.87	0.200	0.55	0.270	0.82
39	0.226	0.86	0.230	0.57	0.340	0.93
40	---	--	0.344	0.83	0.333	0.88
41	---	--	0.541	0.77	0.269	0.75
42	---	--	0.216	0.76	0.207	0.52
43	0.313	0.80	0.235	0.84	0.252	0.84
44	0.347	0.83	0.384	0.84	0.365	0.93

* values calculated from the chromatographic data for uric acid

must be greater than 0.514 (69) for the linear correlation between $\ell n\langle C_i' \rangle_2$ and time to have a 95% probability that it did not occur by chance. The calculated correlation coefficients listed in Table 5 were all greater than 0.514; therefore, the values of σ_i for each monitored constituent can be considered constant. This is consistent with the development of the predictive model.

Three other observations can also be made from Table 5. First, eight constituents that were detected by chromatography in treatments 2 and 3 were not detected in treatment 1. This could possibly be due to the differences in the body-fluid constituents between the two patients. Second, values of σ_i for twenty-six of the forty-seven monitored constituents varied significantly in the three treatments. Figure 10 is an example of a two fold difference in the σ_i's calculated for peak 14 during dialysis treatments 2 and 3. These variations in σ_i could possibly be caused by differences between the CDAK's used in each treatment and/or by differences in the patients themselves. Third, the values of σ_i for uric acid determined from the chromatographic data were within 3% of the values determined from the Dow Diagnostest-concentration data. This indicates that the change in the height of the uric acid peak was directly proportional to the change in uric acid concentration.

It should be emphasized that even though there were variations in the σ_i's of many constituents, the relationship between $\ell n\langle C_i' \rangle_2$ and dialysis time was linear for all the monitored constituents. Thus, the binary, steady-state, mass-transfer relationships used in develop-

ing the predictive model were found to be valid for each of the forty-seven monitored components.

Dialyzer Area Effect on Mass Transfer

Data obtained from the hemodialysis treatments of six uremic patients were used to determine if there was a reduction in mass-transfer area during dialysis and to correlate the fraction of the dialyzer area available for mass transfer to measurable parameters. The hemodialysis conditions and clinical data for these dialysis treatments are listed in Tables 6 and 7 respectively. The blood concentrations of urea and creatinine determined from Dow Diagnostests (19, 20, 21) had an error range of ± 5%.

To determine if there was a significant decrease in mass-transfer area between the dialysis treatments, the actual dialysances for urea and creatinine were compared to the dialysances reported in the literature (17). The actual urea and creatinine dialysances during the hemodialysis treatments of the six uremic patients were calculated by

$$(D_{u,c})_{calc} = \frac{Q_B[\langle C_{u,c}\rangle_1 - \langle C_{u,c}\rangle_2]}{\langle C_{u,c}\rangle_1} \qquad (31)$$

where $(D_{u,c})_{calc}$ = urea or creatinine dialysance calculated from the experimental data

Q_B = volumetric blood flow rate

$\langle C_{u,c}\rangle_1$ = integral average inlet blood concentration of urea or creatinine

$\langle C_{u,c}\rangle_2$ = integral average outlet blood concentration of urea or creatinine.

TABLE 6

OPERATING CONDITIONS FOR THE HEMODIALYSIS

TREATMENTS OF SIX UREMIC PATIENTS

Patient	Q_B (ml/min)	Q_D (ml/min)	Time (min)	$(\Delta P)^*_{obs}$ (mm Hg)	P^*_{uf} (mm Hg)
FD	180	550	210	50/53	235/209
RM	185	525	180	47/51	369/328
MR	210	525	275	20/20	345/255
AR	200	550	175	24/25	153/138
RMC	180	550	180	53/55	283/300
MG	180	500	180	30/33	270/309

* Values at t_o/Values at t_f

Q_B = Blood flow rate

Q_D = Dialysate flow rate

$(\Delta P)_{obs}$ = Observed pressure drop across the CDAK

P_{uf} = Ultrafiltration pressure

t_o = Beginning of the sampling period

t_f = End of the sampling period

TABLE 7

CLINICAL DATA FOR THE HEMODIALYSIS TREATMENTS

OF SIX UREMIC PATIENTS

Clinical Data	Patient FD	RM	MR	AR	RMC	MG
Beginning of the Sampling Period						
Arterial BUN (mg %)*	27.8	35.6	48.0	25.8	40.5	39.9
Venous BUN (mg %)*	8.9	10.5	15.8	5.7	10.6	11.3
Arterial creatinine (mg %)*	4.4	4.8	9.3	6.6	5.0	11.6
Venous creatine (mg %)*	1.7	2.3	3.4	2.7	2.3	4.5
Hematocrit (vol %)	31.5	35.5	14.8	25.3	38.5	20.1
End of the Sampling Period						
Arterial BUN (mg %)*	17.6	20.5	21.0	--	24.3	20.0
Venous BUN (mg %)*	7.1	8.0	4.9	5.5	7.9	5.5
Arterial creatinine (mg %)*	2.5	3.4	4.7	4.4	3.6	7.0
Venous creatinine (mg %)*	1.3	1.3	2.0	--	1.4	2.2
Hematocrit (vol %)	34.3	37.1	14.8	25.5	40.0	19.5

* Blood concentrations are within ± 5 % of the experimental values.

Table 8 lists these calculated and reported dialysances. Comparing these dialysances, all of the calculated dialysances for urea and creatinine were less than the respective reported dialysances. This difference was interpreted as a decrease in mass-transfer area because the reported dialysances were determined in vitro and are for 100% of the CDAK area available for mass transfer. These data also illustrated that the decrease in dialysances was not the same during a dialysis treatment or between the dialysis treatments. This indicates that the mass-transfer rates of urea and creatinine can vary during and between hemodialysis treatments which could possibly be due to changes in the mass-transfer area.

The data in Tables 6, 7, and 8 and equation (31) were used to calculate the apparent fraction of the CDAK area which was available for mass transfer and to compare these values to the area correction factors calculated from equation (28). The area correction factors obtained from this equation were calculated using the blood flow rate, hematocrit, and the observed pressure drop across the CDAK (see Appendix I). Since the literature dialysances of urea and creatinine are for 100% of the CDAK's area available for mass transfer, the ratio of the calculated dialysances to the reported dialysances would be equal to the fraction of the CDAK area available for mass transfer. These ratios were calculated by

$$\alpha_{u,c} = \frac{(D_{u,c})_{calc}}{D_{u,c}} \qquad (32)$$

TABLE 8

CALCULATED AND REPORTED DIALYSANCES (17) OF UREA AND CREATININE FOR THE HEMODIALYSIS TREATMENTS OF SIX UREMIC PATIENTS

Patient	$(D_u)^*_{calc}$ (ml/min)	D_u (ml/min)	$(D_c)^*_{calc}$ (ml/min)	D_c (ml/min)
FD	122/107	149	110/86	127
RM	130/113	151	96/114	129
MR	141/161	163	133/121	136
AR	156/---	159	118/---	133
RMC	129/131	149	110/123	127
MG	133/121	149	97/110	127

* Dialysance at t_o/Dialysance at t_f

where $\alpha_{u,c}$ = fraction of the CDAK area available for mass transfer

$(D_{u,c})_{calc}$ = dialysance of urea or creatinine calculated from the experimental data

$D_{u,c}$ = dialysance of urea or creatinine reported in the literature (17).

Table 9 lists the area correction factors calculated by equation (28), α, and the ratio of the urea dialysances, α_u, and the ratio of the creatinine dialysances, α_c. The ± 20% error limits on α_u and α_c are due to the error limits reported in the Dow Diagnostests (19, 20, 21) and from the error limits on the literature dialysances (17). The data in Table 9 illustrate that 9 out of 11 of the area correction factors calculated by equation (28) where within the error limits associated with α_u and α_c. Also, the values for α_u and α_c for each treatment were within their experimental error limits. From these data, the fraction of the CDAK area which was available for mass transfer could be calculated from the blood flow rate, the patient's hematocrit, and the observed pressure drop across the CDAK which are all measurable parameters. These data also indicate that there is a decrease in mass-transfer area which signficantly affects the mass transfer of dialyzable constituents.

Ultrafiltration Effect on Mass Transfer

The data listed in Tables 6 and 7 were also used to estimate the effect of ultrafiltration on the mass-transfer rates of urea and creatinine. Before the dialysances of urea and creatinine could be compared to ultrafiltration pressure, each of the calculated dialy-

TABLE 9

AREA CORRECTION FACTORS FOR THE HEMODIALYSIS

TREATMENTS OF SIX UREMIC PATIENTS

Patient	Area Correction Factors at the Beginning of the Sampling Period			Area Correction Factors at the End of the Sampling Period		
	α	α_u	α_c	α	α_u	α_c
FD	0.67	0.82±0.16	0.87±0.17	0.71	0.72±0.14	0.68±0.14
RM	0.86	0.86±0.17	0.74±0.15	0.85	0.75±0.15	0.88±0.18
MR	0.95	0.87±0.17	0.98±0.20	0.95	0.99±0.20	0.89±0.18
AR	1.00	0.98±0.20	0.89±0.18	1.00	---	---
RMC	0.85	0.89±0.18	0.76±0.15	0.88	0.81±0.16	0.87±0.17
MG	0.68	0.87±0.17	0.87±0.17	0.60	0.88±0.18	0.98±0.20

sances must be at the same blood flow rate and mass-transfer area. This was accomplished by calculating an effective dialysance at a blood flow rate of 200 ml/min and at 100% of the CDAK area available for mass transfer for each of the dialysis treatments. These effective dialysances were calculated by

$$\bar{\bar{D}}_{u,c} = \left[\frac{(D_{u,c})_{calc}}{\alpha}\right]\left[\frac{(D_{u,c})_{Q_B}}{(D_{u,c})_{200}}\right] \qquad (33)$$

where $\bar{\bar{D}}_{u,c}$ = effective dialysance for urea or creatinine at a blood flow rate of 200 ml/min and for 100% of the CDAK area available for mass transfer

$(D_{u,c})_{calc}$ = urea or creatinine dialysance calculated at the actual hemodialysis conditions

$(D_{u,c})_{Q_B}$ = urea or creatinine dialysance at the actual hemodialysis conditions reported in the literature

$(D_{u,c})_{200}$ = urea or creatinine dialysance at a blood flow rate of 200 ml/min reported in the literature

α = area correction factor calculated from equation (28).

Figures 11 and 12 are plots of the effective dialysances of urea and creatinine versus ultrafiltration pressure. These figures illustrate that there was no correlation between the mass-transfer rate of urea or creatinine with respect to ultrafiltration pressure. This is also consistent with the finding of other investigators (52). The error limits associated with each effective dialysance were due to the error limits in the Dow Diagnostests (19, 20, 21). Since there was no correlation between the effective dialysance and ultrafiltration, the mass transfer of urea and creatinine in the CDAK is diffusion

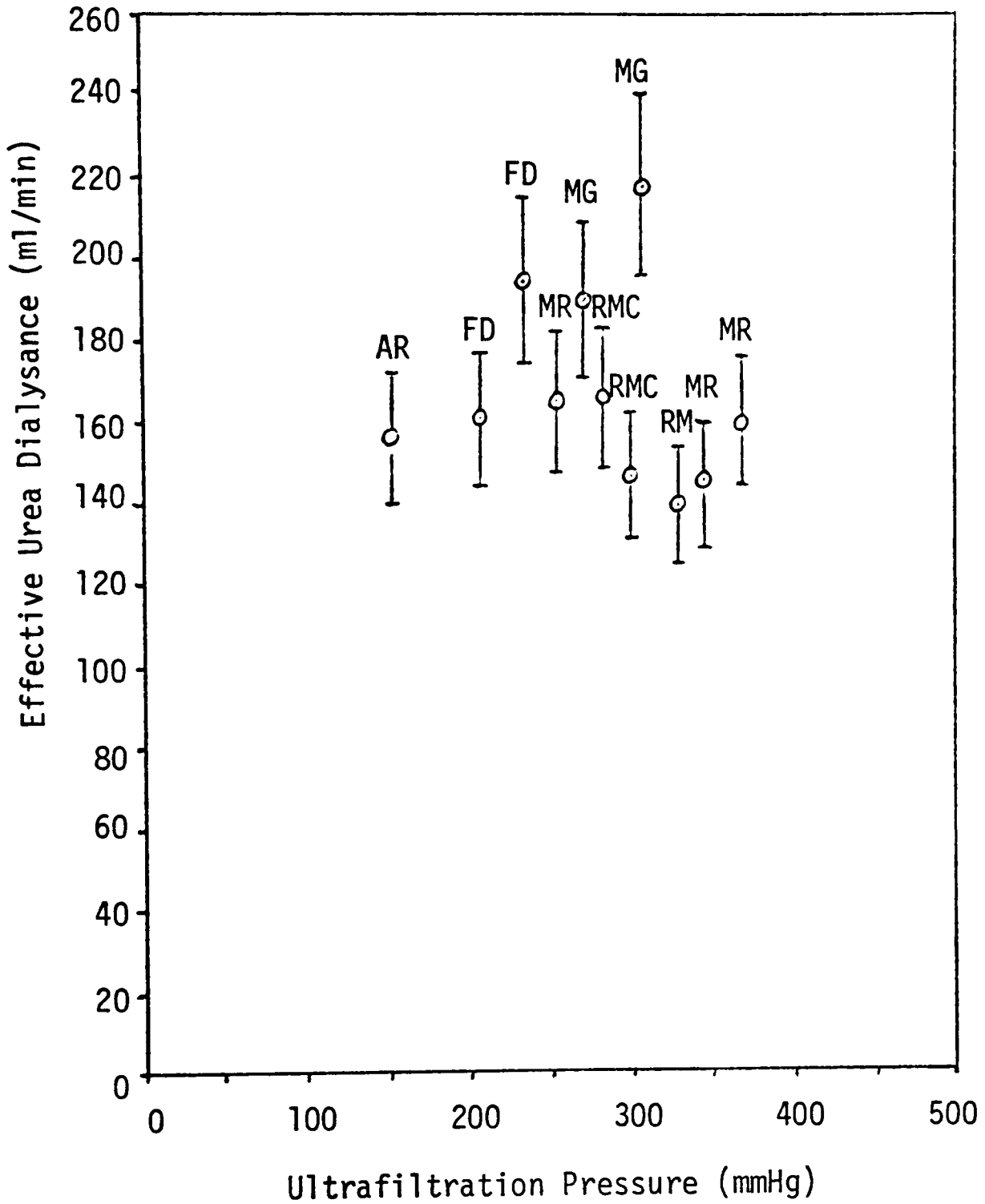

Figure 11. Effect of ultrafiltration pressure on the mass transfer of urea.

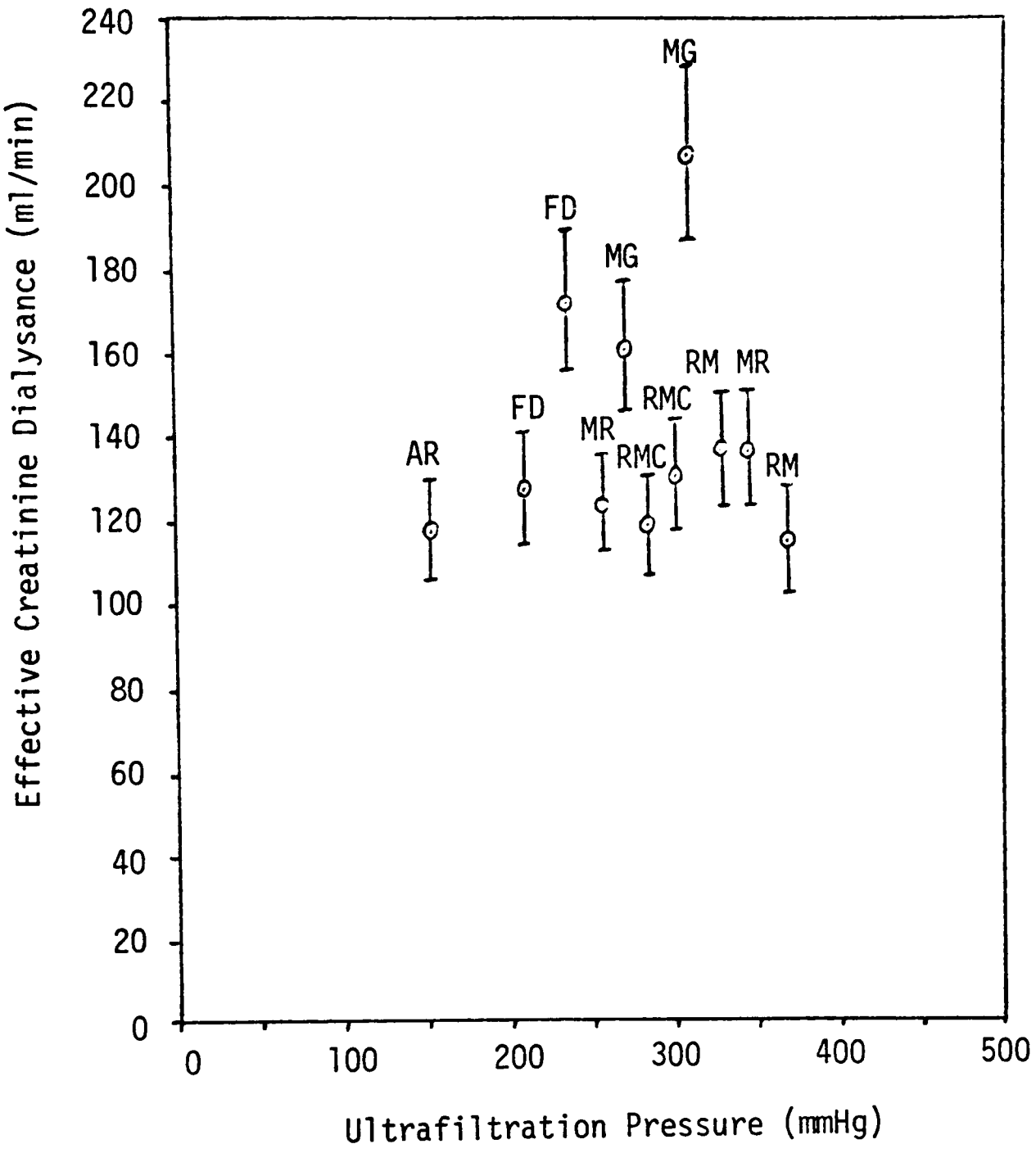

Figure 12. Effect of ultrafiltration pressure on the mass transfer of creatinine.

limited and the ultrafiltration correction factor, η_i, in the model is unity.

Figures 11 and 12 also indicate that there may be significant differences between the CDAK's and/or the uremic patients themselves which caused the differences in the mass-transfer rates of urea and creatinine. This was also indicated by the variations between the σ_i's for the same dialyzed constituent listed in Table 5.

Prediction of Removal Fractions

The data in Tables 6 and 7 were used to compare the removal fractions for urea and creatinine predicted by the model to the observed removal fractions. The observed removal fractions for urea and creatinine were calculated by

$$(E_{u,c})_{obs} = 1 - \frac{\langle C_{u,c} \rangle_{t_f}}{\langle C_{u,c} \rangle_{t_o}} \qquad (34)$$

where $(E_{u,c})_{obs}$ = observed removal fraction of urea or creatinine calculated from the experimental data

$\langle C_{u,c} \rangle_{t_o}$ = body-fluid pool urea or creatinine concentration at the beginning of the sampling interval

$\langle C_{u,c} \rangle_{t_f}$ = body-fluid pool urea or creatinine concentration at the end of the sampling interval.

The variables used to calculate the removal fractions of urea and creatinine from the predictive model are listed in Table 10. Since the fluid volumes of the experimental subjects were unknown, it was necessary to estimate them using the integral form of equation (30).

TABLE 10

MODEL VARIABLES USED TO CALCULATE THE REMOVAL FRACTION OF UREA AND CREATININE

Patient	Fluid Volume (l)	Dialysis Time (min)	α	D_u (ml/min)	D_c (ml/min)
FD	52.8	210	0.69	149	127
RM	38.4	180	0.86	151	129
MR	42.3	275	0.95	163	136
AR	55.6	175	1.00	159	133
RMC	44.8	180	0.87	149	127
MG	33.9	180	0.64	149	127

This expression is

$$V = - \frac{(D_u)_{calc}\, t}{\ell n[\frac{<C_u>_{t_f}}{<C_u>_{t_o}}]} \qquad (35)$$

where V = total fulid volume

$(D_u)_{calc}$ = urea dialysance calculated from the experimental data

t = dialysis time

$<C_u>_{t_o}$ = body-fluid pool urea concentration at the beginning of the sampling interval

$<C_u>_{t_f}$ = body-fluid pool urea concentration at the end of the sampling interval.

The area correction factors listed in Table 10 were calculated from equation (28). The dialysances for urea and creatinine were obtained from the Cordis Dow literature (17). Table 11 lists the urea and creatinine removal fractions calculated by the model and the removal fractions calculated from the experimental data. The error limits on the observed removal fractions were due to the errors associated with the Dow Diagnostests (19, 20). Comparing the data in Table 11, eight of the predicted removal fractions were within the error limits (± 10%) of the observed removal fractions and two predicted values were within ± 13% of the observed values. Only two predicted removal fractions deviated significantly (± 20%) from the observed values. These data indicate that this model can be used to predict the removal fractions of urea and creatinine for given hemodialysis conditions, component dialysances, patient-fluid volume, and dialysis time.

TABLE 11

REMOVAL FRACTIONS OF UREA AND CREATININE FOR THE HEMODIALYSIS TREATMENTS OF SIX UREMIC PATIENTS

Patient	$(E_u)_{obs}$	$(E_u)_{calc}$	$(E_c)_{obs}$	$(E_c)_{calc}$
FD	0.37±0.04	0.34	0.29±0.03	0.29
RM	0.42±0.04	0.46	0.37±0.04	0.41
MR	0.56±0.06	0.63	0.49±0.05	0.57
AR	0.36±0.04	0.39	0.33±0.03	0.34
RMC	0.40±0.04	0.41	0.38±0.04	0.36
MG	0.50±0.05	0.40	0.40±0.04	0.35

Clinical data reported by Gotch, et al. (30) for nineteen uremic patients were also used to compare predicted and observed removal fractions for urea and creatinine. Table 12 lists these removal fractions and an area correction factor. Using equation (29), these area correction factors were calculated by

$$\alpha_{u,c} = \frac{V\ \ell n\ [1 - (E_{u,c})_{obs}]}{D_{u,c}\ t} \qquad (36)$$

where $\alpha_{u,c}$ = area correction factor calculated from the observed removal fractions for urea or creatinine

V = patient-fluid volume

$(E_{u,c})_{obs}$ = observed removal fraction for urea or creatinine

$D_{u,c}$ = dialysance of urea or creatinine reported in the literature

t = dialysis time.

These data in Table 11 illustrate that there was up to a 59% decrease in the mass transfer of urea and creatinine which was possibly due to a decrease in mass-transfer area in the CDAK. This explaination is consistent with the decrease in mass-transfer rates of urea and creatinine observed from the hemodialysis treatments of the six uremic patients used in this investigation.

TABLE 12

AREA CORRECTION FACTORS AND UREA AND CREATININE REMOVAL FRACTIONS FOR THE HEMODIALYSIS TREATMENTS OF NINETEEN UREMIC PATIENTS FROM THE DATA REPORTED BY GOTCH, et al. (30)

Patient Number	$(E_u)_{calc}$	$(E_u)_{obs}$ ±10%	$(E_c)_{calc}$	$(E_c)_{obs}$ ±10%	α_u ±10%	α_c ±10%
1	0.77	0.55	0.70	0.44	0.55	0.48
2	0.78	0.58	0.70	0.51	0.58	0.59
3	0.71	0.65	0.65	0.57	0.86	0.80
4	0.75	0.50	0.68	0.40	0.50	0.44
5	0.64	0.42	0.58	0.46	0.53	0.71
6	0.77	0.63	0.71	0.52	0.67	0.59
7	0.83	0.66	0.77	0.58	0.61	0.58
8	0.75	0.71	0.68	0.46	0.90	0.55
9	0.76	0.73	0.68	0.67	0.92	0.96
10	0.76	0.64	0.69	0.53	0.72	0.65
11	0.73	0.65	0.68	0.44	0.80	0.51
12	0.85	0.69	0.78	0.49	0.62	0.43
13	0.71	0.51	0.64	0.51	0.57	0.70
14	0.80	0.58	0.74	0.56	0.53	0.61
15	0.82	0.64	0.75	0.51	0.60	0.52
16	0.67	0.37	0.60	0.50	0.41	0.75
17	0.65	0.47	0.59	0.45	0.50	0.68
18	0.62	0.50	0.56	0.45	0.72	0.73
19	0.74	0.57	0.67	0.51	0.63	0.64

CHAPTER 10

HEMODIALYSIS TREATMENT PROGRAMS FOR UREMIC PATIENTS

From the results of this investigation, the predictive model can be used as a basis for developing individual hemodialysis programs for uremic patients. By specifying the hemodialyzer operating conditions and the removal fraction of a dialyzed constituent, this model can be used to predict the dialysis time required to meet these specifications. Nomograms for equation (A3) and the predictive model, shown in Figures 13 and 14 respectively, were constructed to aid the dialysis personnel in using the model for hemodialysis therapy. The following hypothetical examples explain how to use Figures 13 and 14 for the hemodialysis treatments of uremic patients.

Example 1: Table 13 is an example hemodialysis program for a uremic patient developed using Figures 13 and 14. The patient data includes the total fluid volume, hematocrit, and average predialysis creatinine concentration. The blood and dialysate flow rates are specified before dialysis; however, the pressure drop across the CDAK is determined after a steady blood flow through the artificial kidney has been achieved. The creatinine removal fraction in this example was specified to decrease the body-fluid creatinine concentration from 10 mg% to 5 mg%. The specified amount of water that needs to be removed is determined by the weight gain of the patient since his last dialysis treatment. The calculated pressure drop across the CDAK, $(\Delta P)_{calc}$, is obtained from Figure 13 by knowing

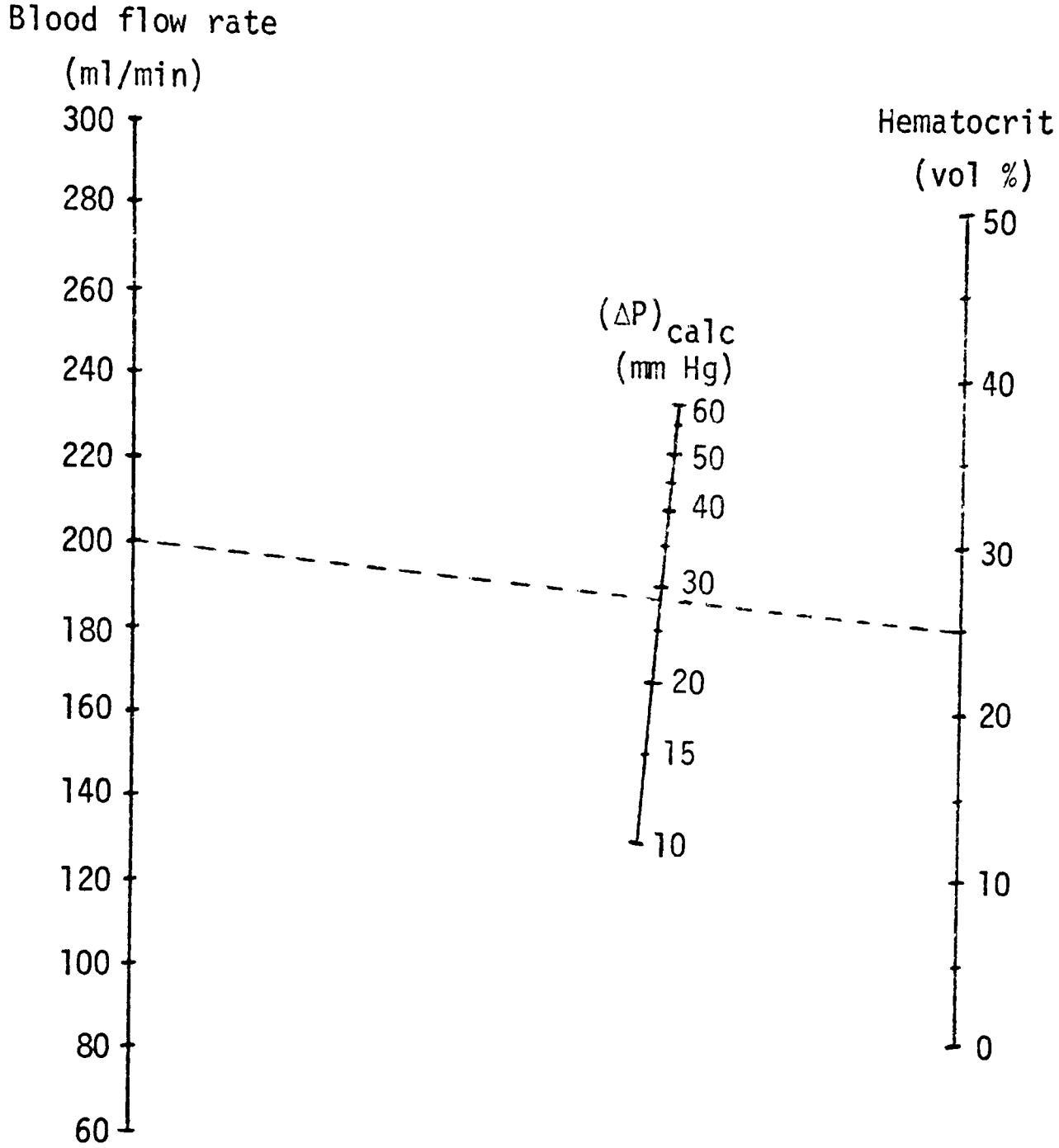

Figure 13. Nomogram for equation (A3).

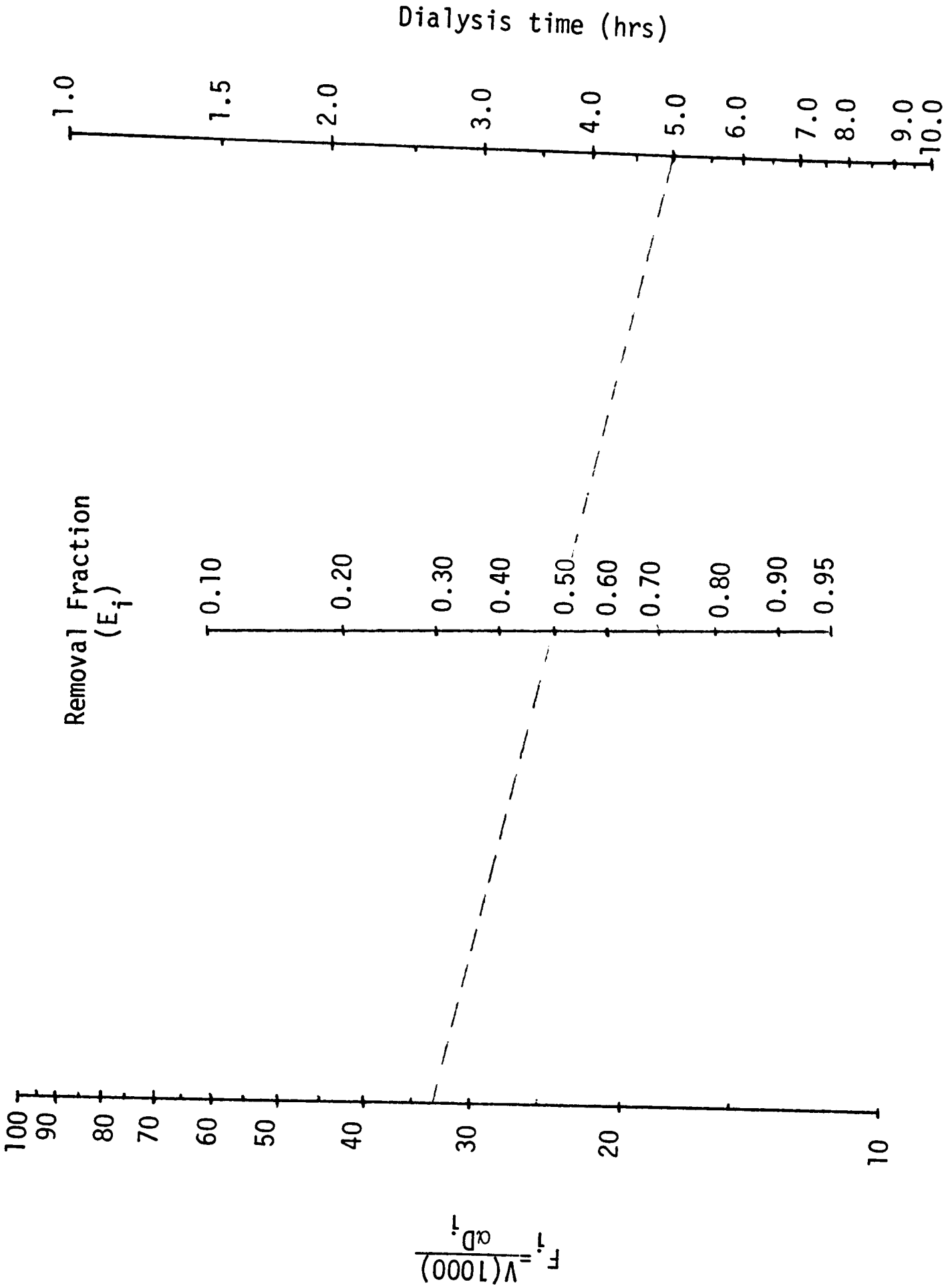

Figure 14. Nomogram for the predictive model.

TABLE 13

HEMODIALYSIS PROGRAM FOR EXAMPLE 1

Patient Data	Value
Total fluid volume	40 l
Hematocrit	25 vol %
Average predialysis creatinine blood concentration	10 mg %
Hemodialyzer Operating Conditions	
Blood flow rate	200 ml/min
Dialysate flow rate	500 ml/min
Pressure drop across the CDAK	30 mm Hg
Specified Values	
Creatinine removal fraction	0.50
Total water removal	2 lbs
Calculated Values	
Pressure drop across the CDAK, $(\Delta P)_{calc}$	27.9 mm Hg
Area correction factor, α	0.93
Creatinine dialysance, D_c	133 ml/min
$F_c = V(1000)/(\alpha D_c)$	32.3
Dialysis time	5.0 hrs
Ultrafiltration pressure	180 mm Hg

the blood flow rate and hematocrit. To obtain this value from Figure 13, a straightedge is placed on the values for blood flow rate and hematocrit and the calculated pressure drop is read where the straightedge intersects the $(\Delta P)_{calc}$ line. The area correction factor, α, can then be calculated by

$$\alpha = \frac{(\Delta P)_{calc}}{(\Delta P)_{obs}} \tag{37}$$

where α = area correction factor

$(\Delta P)_{calc}$ = pressure drop across the CDAK obtained from Figure 13

$(\Delta P)_{obs}$ = observed pressure drop across the CDAK during hemodialysis.

The dialysance for creatinine is obtained from the Cordis Dow literature (17). The dialysis time required to meet these specified parameters is obtained from Figure 14. To use Figure 14, the value for F_c is calculated by

$$F_c = \frac{V(1000)}{\alpha\, D_c} \tag{38}$$

where F_c = nomogram parameter for creatinine (hrs)

V = patient fluid volume (l)

α = area correction factor calculated from equation (37)

D_c = creatinine dialysance reported in the literature.

Once F_c has been determined, the dialysis time can be obtained from Figure 14 by placing a straightedge on the calculated value for F_c and the specified removal fraction and by reading the dialysis time

where the straightedge intersects the dialysis-time line. After obtaining the dailysis time, the ultrafiltration pressure required to remove the specified amount of water from the patient can be calculated from the Cordis Dow literature (17). In this example, the dialysis time required to decrease the creatinine concentration from 10 mg% to 5 mg% would be five hours at the specified hemodialyzer operating conditions.

Example 2: Table 14 is the hemodialysis program for this example. The only difference in the patient data, hemodialysis operating conditions, and specified values between Tables 13 and 14 is the fluid volume This example illustrates that for a patient having a 30 liter fluid volume, 3.6 hours of dialysis time is required to remove the same fraction of creatinine. This is 1.4 hours less than the time required for a patient with a 40 liter fluid volume. It should also be emphasized that in order to remove the same amount of water, the ultrafiltration pressure must be increased from 180 mm Hg to 252 mm Hg because of the shorter dialysis time.

Example 3: Table 15 is the hemodialysis program for this example. The only difference between this example and example 1 is an increase in the observed pressure drop across the CDAK from 30 mm Hg to 35 mm Hg. This 5 mm Hg increase in pressure drop increases the dialysis time to 5.8 hours required to remove the same amount of creatinine specified in example 1. This increase in dialysis time is due to a decrease in mass-transfer area which is indicated by a higher $(\Delta P)_{obs}$.

TABLE 14

HEMODIALYSIS PROGRAM FOR EXAMPLE 2

Patient Data	Value
Total fluid volume	30 l
Hematocrit	25 vol %
Average predialysis creatinine blood concentration	10 mg %
Hemodialyzer Operating Conditions	
Blood flow rate	200 ml/min
Dialysate flow rate	500 ml/min
Pressure drop across the CDAK	30 mm Hg
Specified Values	
Creatinine removal fraction	0.50
Total water removal	2 lbs
Calculated Values	
Pressure drop across the CDAK, $(\Delta P)_{calc}$	27.9 mm Hg
Area correction factor, α	0.93
Creatinine dialysance, D_c	133 ml/min
$F_c = V(1000)/(\alpha D_c)$	24.3
Dialysis time	3.6 hrs
Ultrafiltration pressure	252 mm Hg

TABLE 15

HEMODIALYSIS PROGRAM FOR EXAMPLE 3

Patient Data	Value
Total fluid volume	40 l
Hematocrit	25 vol %
Average predialysis creatinine blood concentration	10 mg %
Hemodialyzer Operating Conditions	
Blood flow rate	200 ml/min
Dialysate flow rate	500 ml/min
Pressure drop across the CDAK	35 mm Hg
Specified Values	
Creatinine removal fraction	0.50
Total water removal	2 lbs
Calculated Values	
Pressure drop across the CDAK, $(\Delta P)_{calc}$	27.9 mm Hg
Area correction factor, α	0.80
Creatinine dialysance, D_c	133 ml/min
$F_c = V(1000)/(\alpha D_c)$	37.8
Dialysis time	5.8 hrs
Ultrafiltration pressure	180 mm Hg

These three examples illustrate the use of Figures 13 and 14 in developing hemodialysis programs for uremic patients. They also illustrate that a hemodialysis program should be developed for each individual patient due to the effect of body-fluid volume on dialysis time. The last example illustrates the necessity of accurately monitoring the pressure drop across the kidney because of the effect mass-transfer area has on the dialysis time.

CHAPTER 11

LIMITATIONS

The following limitations were imposed on the validity of the results and conclusions of this investigation:

1. The following assumptions were incorporated in the development of the expression for the mass flux of a solute at any point along the CDAK membrane: (a) the dialyzable solutes are in small concentrations in the blood, (b) the mass flux of each solute can be approximated by a binary, steady-state relation, (c) blood is a homogeneous fluid with constant density and viscosity, (d) water makes up the majority of the blood constituents, (e) the r-directional mass flux of water is much greater than the r-directional mass flux of the dialyzable constituents, (f) a constant fraction of a solute in the bulk blood phase is transmitted to the blood-membrane interface by bulk flow in the r-direction, (g) a constant fraction of the solute in the dialysate at the dialysate-membrane interface is transmitted to the bulk dialysate by bulk flow in the r-direction, (h) the diffusive mass flux of a solute occurs only in the r-direction, (i) the major blood- and dialysate-side resistances to mass transfer occur across thin, stag-

nant films, (j) the diffusivities of the solutes are constant in the blood, membrane, and dialysate, (k) the thickness of the blood and dialysate films are much less than the distance from the center of the fiber to the blood and dialysate films, (l) the membrane thickness is much less than the inside radius of the fiber, (m) the concentration of each solute at the fluid-membrane interfaces can be related to the membrane surface concentrations by an equilibrium coefficient, (n) the fluid-membrane interface equilibrium coefficient is the same for both sides of the membrane, (o) the blood concentration of a solute at the blood-membrane interface can be related to the bulk blood concentration by a constant, (p) the dialysate-side membrane surface concentration of a solute can be related to the blood-side membrane surface concentration by a constant, (q) the bulk dialysate concentration of a solute is much less than the bulk blood concentration, and (r) the mass flux of a solute is slow.

2. The following assumptions were incorporated in the development of the predictive model: (a) the body-fluid pools can be treated as a constant-volume, well-mixed pool, (b) the outlet blood concentration of a solute is constant in the blood tubing from the CDAK to the body-fluid pool, (c) the blood concentration

of a solute entering the CDAK is equal to the concentration of the solute in the body-fluid pool, (d) the concentration of a solute is constant in the tubing from the body-fluid pool to the CDAK, (e) the outlet dialysate concentration of a solute is constant in the tubing leaving the CDAK, (f) the dialysate flow is single pass, (g) the volume of the body-fluid pool is much greater than the volume inside the blood tubing and the CDAK, (h) the change in solute concentration in the body-fluid pool is much less than the change in solute concentration inside the CDAK, (i) there is no accumulation of a solute in the CDAK, (j) the mass transfer of a solute can be approximated by a binary, steady-state relation, (k) the overall mass-transfer coefficient is constant, (l) the overall ultrafiltration coefficient is constant, (m) the total mass-transfer area is constant, and (n) the solute dialysance, blood and dialysate flow rates, membrane properties, and ultrafiltration pressure are constant during dialysis.

3. The concentration of urea, creatinine, and uric acid evaluated by Dow Diagnostests had an error of ± 5%.
4. Only the Model 4, Cordis Dow Artificial Kidney was used in this investigation.

5. It was assumed that there was no degradation of dialyzed constituents during vacuum evaporation and storage.
6. The constituents monitored by anion-exchange chromatography were limited to components which absorbed ultraviolet light at 254 nm and 280 nm.
7. It was assumed that the change in concentration of the constituents monitored by chromatography was directly proportional to the change in peak height.
8. The following assumptions were made in calculating an expected pressure drop across the CDAK: (a) blood is a homogeneous, incompressible fluid, (b) laminar, Newtonian flow exists in the fibers, (c) there is no slip at the fiber wall, (d) the shear stress depends only on shear rate, and (e) end effects are negligible.
9. The calculated pressure drop across the CDAK can only be used for hematocrits ranging from 15 vol% to 35 vol% and for blood flow rates ranging from 100 ml/min to 300 ml/min.

CHAPTER 12

CONCLUSIONS

Based on the experimental results of this investigation which are subject to the study's limitations, the following conclusions were reached:

1. The concentration-time data obtained for forty-seven dialyzed constituents indicated that the mass-transfer rate of each constituent could be described by the binary, steady-state relationships used in developing the predictive model.
2. The decrease in mass-transfer area was found to significantly affect the mass-transfer rate of urea and creatinine.
3. The decrease in mass-transfer area was correlated to blood flow, hematocrit, and pressure drop across the CDAK.
4. The decrease in mass-transfer area was not consistent during or between hemodialysis treatments.
5. The mass transfer of urea and creatinine in the CDAK was found to be diffusion limited.
6. The mass-transfer rates of the monitored constituents varied between hemodialysis treatments and between the uremic patients themselves.
7. Eight of the twelve removal fractions for urea and creatinine calculated from the predictive model were within the error limits of the actual removal fractions.

CHAPTER 13

RECOMMENDATIONS

From the results of this investigation, the following recommendations are suggested for further study:

1. In order to separate the CDAK and patient variables which possibly affect mass transfer, in-vitro and in-vivo mass-transfer data need to be obtained from the same CDAK.
2. The predictive model needs to be extended to other artificial kidneys.
3. The predictive model needs to be further evaluated as a basis for individual hemodialysis treatment programs and as a possible basis for a control unit for hemodialysis machines.
4. The dialyzed constituents monitored by chromatography need to be identified. To achieve this, better resolution of the eluted constituents is required and a different buffer system needs to be developed.

NOMENCLATURE

Symbols

A_T = total mass transfer area in the CDAK with respect to the inside diameter of the fibers

b = intercept calculated from the regression analysis of HCT versus $\ln(\Delta P)$

C_i = concentration of "i" in the blood

$\bar{C}_i$ = integral average bulk concentration of "i" in the blood

$\bar{C}'_i$ = integral average bulk concentration of "i" in the dialysate

$\langle C_i \rangle_1$ = integral average blood concentration of "i" entering the CDAK

$\langle C_i \rangle_2$ = integral average blood concentration of "i" exiting the CDAK

$\langle C'_i \rangle_2$ = integral average dialysate concentration of "i" exiting the CDAK

$\Delta\langle \bar{\bar{C}}_i \rangle_{lm}$ = effective logarithemic-mean concentration driving force in the CDAK

$\langle \bar{\bar{C}}_i \rangle_1$ = effective blood concentration of "i" entering the CDAK

$\langle \bar{\bar{C}}_i \rangle_2$ = effective blood concentration of "i" exiting the CDAK

C_{im} = concentration of "i" in the blood at the blood-membrane interface

C'_{im} = concentration of "i" in the dialysate at the dialysate-membrane interface

$(C_{im})_B$ = concentration of "i" on the blood-side membrane surface

$(C_{im})_D$ = concentration of "i" on the dialysate-side membrane surface

$\langle C_u \rangle_{t_o}$ = body fluid pool urea concentration at the beginning of the sampling interval

$\langle C_u \rangle_{t_f}$ = body fluid pool urea concentration at the end of the sampling interval

$\langle C_{u,c} \rangle_1$ = integral average inlet blood concentration of urea or creatinine

$\langle C_{u,c} \rangle_2$ = integral average outlet blood concentration of urea or creatinine

$\langle C_{u,c} \rangle_{t_o}$ = body fluid pool urea or creatinine concentration at the beginning of the sampling interval

$\langle C_{u,c} \rangle_{t_f}$ = body fluid pool urea or creatinine concentration at the end of the sampling interval

D_c = creatinine dialysance reported in the literature

D_{id} = dialysance of "i" due to diffusion

D_{iT} = total dialysance of "i"

D_{iuf} = dialysance of "i" due to ultrafiltration

D_u = urea dialysance reported in the literature

$(D_u)_{calc}$ = urea dialysance calculated from the experimental data

$D_{u,c}$ = urea or creatinine dialysance reported in the literature

$\bar{\bar{D}}_{u,c}$ = effective dialysance of urea or creatinine

$(D_{u,c})_{calc}$ = urea or creatinine dialysance calculated from the experimental data

$(D_{u,c})_{Q_B}$ = urea or creatinine dialysance at the actual hemodialysis conditions reported in the literature

$(D_{u,c})_{200}$ = urea or creatinine dialysance at a blood flow rate of 200 ml/min reported in the literature

$\mathcal{D}_{iB}$ = diffusivity of "i" in the blood

$\mathcal{D}_{im}$ = diffusivity of "i" in the membrane

d = fiber diameter

E_i = fraction of "i" in the body fluid pool removed during dialysis

$(E_c)_{calc}$ = removal fraction of creatinine calculated from the predictive model

$(E_c)_{obs}$ = observed removal fraction of creatinine

$(E_u)_{calc}$ = removal fraction of urea calculated from the predictive model

$(E_u)_{obs}$ = observed removal fraction of urea

$(E_{u,c})_{obs}$ = observed removal fraction of urea or creatinine

F_c = nomogram parameter for creatinine in Figure 14

F_i = nomogram parameter for "i" in Figure 14

f = unity with units of mm Hg

HCT = blood hematocrit

K_i = local overall mass transfer coefficient for "i" at any point along the membrane

K_{iT} = overall mass transfer coefficient for "i" in the CDAK

k_i = local mass transfer coefficient for "i" across the stagnant blood film

k_i' = local mass transfer coefficient for "i" across the stagnant dialysate film

k_{im} = local mass transfer coefficient for "i" in the membrane

L = fiber length

L_e = entry length

m = slope calculated from the regression analysis of HCT versus $\ln(\Delta P)$

$\dot{m}_{iT}$ = total mass transfer rate of "i" per pass through the CDAK at any time during hemodialysis

N_B = r-directional mass flux of the blood

N_i = r-directional mass flux of "i" in the blood

N_i' = r-directional mass flux of "i" in the dialysate

$\bar{N}_i$ = r-directional mass flux of "i" at r_1

N_{im} = r-directional mass flux of "i" in the membrane

$(N_i)_{r_o}$ = r-directional mass flux of "i" at r_o

$(N_i)_{r_2}$ = r-directional mass flux of "i" at r_2

$(N_{im})_{r_1}$ = r-directional mass flux of "i" at r_1

N_{iz} = z-directional mass flux of "i" in the blood

N_{iz}' = z-directional mass flux of "i" in the dialysate

N_j = mass flux of each dialyzed constituent

N_{Re} = Reynolds number

N_w = r-directional mass flux of water

P' = pressure in the dialysate side of the CDAK

P_a = blood pressure at the arterial side of the CDAK

P_{im} = permeability of "i" in the membrane

P_v = blood pressure at the venous side of the CDAK

$(\Delta P)_{calc}$ = calculated pressure drop across the CDAK

$(\Delta P)_{obs}$ = observed pressure drop across the CDAK

P_{uf} = ultrafiltration pressure

Q_B = volumetric blood flow rate

Q_D = volumetric dialysate flow rate

R_i = correlation coefficeint for σ_i

r = fiber radius

r_o = distance from the center of the fiber to the stagnant blood film

r_1 = distance from the center of the fiber to the blood-membrane interface

r_2 = distance from the center of the fiber to the dialysate-membrane interface

t = dialysis time

t_o = beginning of the sampling interval

t_f = end of the sampling interval

V = volume of the body fluid pool

v_w = r-directional velocity of water

$\bar{v}_w$ = r-directional velocity of water at r_1

$(v_w)_{r_o}$ = r-directional velocity of water at r_o

$(v_w)_{r_1}$ = r-directional velocity of water at r_1

$(v_w)_{r_2}$ = r=directional velocity of water at r_2

x_i = mass fraction of "i" in the bulk phase moving in the r-direction

Greek Letters

α = area correction factor or the fraction of the dialyzer area available for mass transfer

α_c = area correction factor calculated from the mass transfer data for creatinine

α_u = area correction factor calculated from the mass transfer data for urea

$\alpha_{u,c}$ = area correction factor calculated from the mass transfer data for urea or creatinine

β_i = a constant relating the concentration of "i" in the blood at the blood-membrane interface to the bulk phase blood concentration of "i"

β_{im} = a constant relating the membrane surface concentrations of "i"

Γ_{im} = equilibrium coefficient relating the blood- and dialysate-membrane interface concentrations of "i" to the membrane surface concentrations of "i"

δ_f = thickness of the stagnant blood film

η_i = ultrafiltration correction factor

ϕ_i = local overall ultrafiltration coefficient for "i"

Ψ_i = fraction of "i" in the blood phase transmitted to the blood-membrane interface by bulk flow in the r-direction

Ψ_i' = fraction of "i" in the dialysate at the dialysate-membrane interface transmitted to the bulk dialysate by bulk flow in the r-direction

Ψ_{im} = fraction of "i" on the blood-side membrane surface transmitted through the membrane

σ_i = ratio of the total dialysance of "i" to the volume of the body fluid pool

τ_w = wall shear stress

BIBLIOGRAPHY

1. Able, J.J., Rowntree, L.G., and Turner, B.B.: "The Remvoal of Diffusable Substances from the Circulating Blood by Means of Dialysis", p. 51, vol. 28, Tran. A. Am. Physicians, (1913).

2. Alfrey, A.C.: "Denver Dialysis Disease: A Dilema", p. 17, Med. World News, (May 17, 1974).

3. Asbury, A.K., Victor, M., and Adams, R.P.: "Uremic Poly-neuropathy", pp. 405-428, vol. 8, Arch. Neurol. Psychiat. Chicago, (1963).

4. Babb, A.L., Maurer, C.J., Fry, D.L., Popovich, R.P., and McKee, R.E.: "The Determination of Membrane Permeabilities and Solute Diffusivities with Applications to Hemodialysis", pp. 59-68, vol. 67, Chem. Engr. Prog. Sym. Series, (1972).

5. Babb, A.L., Popovich, R.P., Christopher, T.H., and Scribner, B.H.: "The Genesis of the Square Meter-Hour Hypothesis", pp. 81-91, vol. 17, Am. Soc. Art. Int. Organs, (1971).

6. Bennett, B. and Rosenblum, C.: "Identification of Calcium Oxalate Crystals in the Myocardium in Patients with Uremia", pp. 947-955, vol. 10, Lab. Invest., (1961).

7. Bennington, J.L., Harber, S.L., Smith, J.V., and Warner, N.E.: "Crystals of Calcium Oxalate in the Human Kidney", pp. 8-14, vol. 41, Am. J. Clin. Path., (1964).

8. Breen, M. and Marshall, R.T.: "An Automated Fluorometric Method for the Direct Determination of Magnesium in Serum and Urine Using o-o'-dehydroxyazobenzene: Studies on Normal and Uremic Subjects", pp. 701-712, vol. 68, J. Lab. Clin. Med., (1966).

9. Bonas, J.E., Cohen, B.D., and Natelson, S.: "Separation and Estimation of Certain Guanidino Compounds, Application to Human Urine", pp. 63-67, vol. 17, Microchem. J., (1963).

10. Bright, R.: "Reports of Medical Cases Selected with a View of Illustrating the Symptoms and Care of Diseases by a Reference Morbid Anatomy", vol. 1, Longman, Rees, Orne, Brown, and Green, London, England, (1827).

11. Burtis, C.A.: "The Separation of the Ultraviolet-Absorbing Constituents of Urine by High-Pressure Liquid Chromatography", pp. 97-106, vol. 52, J. Chrom., (Oct. 1970).

12. Burtis, C.A. and Warren, K.S.: "Identification of Urinary Constituents Isolated by Anion-Exchange Chromatography", p. 290, vol. 14, Clin. Chem., (1968).

13. Chicote, D.D. and Mrochek, J.E.: "The Chromatographic Analysis of Naturally Fluorescing Compounds: Rapid Analysis of Nanogram Amounts of Indoles in Physiologic Fluids", ORNL Pub., Oak Ridge, Tenn., (1972).

14. "Chromatography, Electrophoresis, and Membrane Technology", Bio-Rad Laboratories Tech. Lit., Richmond, Calif., (1975).

15. Cohen, B.D.: "Guanidinosuccinic Acid in Uremia", p. 846, vol. 126, Arch. Intern. Med., (1970).

16. Cohen, B.D. and Horowitz, H.I.: "Carbohydrate Metabolism in Uremia: Inhibition of Phosphate Release", pp. 407-413, vol. 21, Am. J. Clin. Nutr., (1968).

17. "Cordis Dow Artificial Kidney: Model 4", p. 5, Cordis Corp. Tech. Lit., Miami, Fa., (1975).

18. Dayan, A.D., Gardner-Thorpe, C., Down, P.F., and Gleadle, R.I.: "Peripheral Neuropathy in Uremia: Pathological Studies on Peripheral Nerves from Six Patients", p. 649, vol. 20, Neurology, (1970).

19. "Dow Diagnostests for Blood Urea Nitrogen Determination", Dow Diagnostests, Indianapolis, Ind., (1975).

20. "Dow Diagnostests for Creatinine Determination", Dow Diagnostests, Indianapolis, Ind., (1975).

21. "Dow Diagnostests for Uric Acid Determination", Dow Diagnostests, Indianapolis, Ind., (1975).

22. Dreyfus, P.M.: "The Regional Distribution of Transketolase in the Normal and in the Thiamine Deficient Nervous System", p. 119, vol. 24, J. Neuropath. Exp. Neurol., (1970).

23. Emerson, P.M. and Wilkinson, J.H.: "Urea and Oxalate Inhibition of Serum Lactate Dehydrohenase", pp. 803-807, vol. 18, J. Clin. Path., (1965).

24. Emerson, P.M., Withycombe, W.A., and Wilkison, J.H.: "Inhibition of Lactate Dehydrogenase of Sera of Uremic Patients", pp. 571-572, Lancet, (1965).

25. Fanger, J. and Esparza, A.: "Crystals of Calcium Oxalate in Kidneys in Uremia", pp. 597-603, vol. 41, Am. J. Clin. Path., (1964).

26. Foster, N.B.: "The Isolation of a Toxic Substance from the Blood of Uremic Patients", pp. 305-308, vol. 30, Trans. Ass. Am. Physns., (1915).

27. Giordano, C., Bloom, J., and Merrill, J.P.: "Effect of Urea on Physiologic Systems, Studies on Monoamine Oxidase Activity", pp. 396-400, vol. 59, J. Lab. Clin. Med., (1962).

28. Giovanetti, S., Biagini, M., Balestri, P.L., Navalesi, R., Giagnoni, P., De Matteis, A., Gerro-Milone, P., and Perfetti, C.: "Uremia-Like Syndrome in Dogs Chronically Intoxicated with Methyguanidine and Creatinine", pp. 445-452, vol. 36, Clin. Sci., (1969).

29. Giovanetti, S., Cioni, L., Balestri, P.L., and Biagini, M.: "Evidence that Guanidine and Some Related Compounds Cause Hemolysis in Chronic Uremia", pp. 141-148, vol. 34, Clin. Sci., (1968).

30. Gotch. F., Lipps, B.J., Weaver, J., Brandes, J., Rosin, J., Sargent, J., Oja, P.D.: "Chronic Hemodialysis with the Hollow Fiber Artificial Kidney", pp. 87-96, vol. 15, Trans. Am. Soc. Art. Int. Organs, (1969).

31. Grollman, E.F. and Grollman, A.: "Toxicity of Urea and Its Role in the Pathogenesis of Uremia", pp. 749-754, vol. 38, J. Clin. Invest., (1959).

32. Haley, E.E., Corcoran, B.J., Dorer, F.D., and Buchanan, D.L.: "B-aspartyl Peptides in Enzymatic Hydrolysates of Protein", p. 3229, vol. 5, Biochem., (1966).

33. Harrison, T.R. and Mason, M.F.: "The Pathogenesis of the Uremic Syndrome", pp. 1-44, vol. 16, Med. Balt., (1937).

34. Hicks, J.M., Young, D.S., and Wooton, I.D.P.: "The Effect of Uremic Blood Constituents on Certain Cerebral Enzymes", pp. 228-235, vol. 9, Clin. Chim. Acta., (1964).

35. Jolley, R.L., Warren, K.S., Scott, C.D., and Freeman, M.L.: "Carbohydrates in Normal Urine and Blood Serum as Determined by High-Resolution Column Chromatography", p. 793, vol. 53, Am. J. Clin. Path., (1970).

36. Katz, S., Dinsmore, S.R., and Pitt, W.W., Jr.: "A Small Automated High-Resolution Analyzer for Determination of Carbohydrates in Body Fluids", p. 131, vol. 17, Clin. Chem., (1971).

37. Kloff, W.J. and Berk, H.T.J.: "The Artificial Kidney: A Dialyzer with a Great Area", p. 121, vol. 117, Acta. Med. Scand., (1944).

38. Kramer, B., Seligon, H., Baltrash, H., and Seligson, D.: "The Isolation of Several Aromatic Acids from the Hemodialysis Fluids of Uremic Patients", pp. 363-371, vol. 2, Clin. Chim. Acta., (1965).

39. Lightfoot, E.N.: "Descriptive Biorheology", Transport Phenomena in Living Systems, pp. 30-38, John Wiley & Sons, New York, N.Y., (1974).

40. Lindner, A. and Curtis, K.: "Morbidity and Mortality Associated with Long-Term Hemodialysis", pp. 143-150, Hosp. Pract., (Nov. 1974).

41. Lonergun, E.T., Semar, M., and Lange, K.: "A Dialyzable Toxic Factor in Uremia", pp. 269-271, vol. 16, Am. Soc. Art. Int. Organs, (1970).

42. Mason, M.F., Resnik, H., Jr., Minot, A.S., Rainey, J., Pilcher, C., and Harrison, T.R.: "Mechanism of Experimental Uremia", pp. 312-336, vol. 60, Archs. Intern. Med., (1937).

43. Merrill, J.F.: The Treatment of Renal Failure: Therapuetic Principles in the Management of Acute Renal Failure, 2nd ed., William Heinamann Medical Books Ltd., London, England, (1965).

44. Mrochek, J.E., Butts, W.C., Rainey, W.T., Jr., and Burtis, C.A.: "Separation and Identification of Urinary Constituents by Use of Multiple Analytical Techniques", pp. 72-77, vol. 17, Clin. Chem., (1972).

45. Mrochek, J.E. and Rainey, W.T., Jr.: "Identification and Biochemical Significance of Substituted Furans in Human Urine", ORNL Pub., Oak, Ridge, Tenn., (1972).

46. Olsen, N.S. and Bassett, J.W.: "Blood Levels of Urea Nitrogen, Phenol, Guanidine, and Creatinine in Uremia", pp. 52-59, vol. 10, Am. J. Med., (1951).

47. Peters, J.H., Gulyassy, P.F., Lin, S.C., Ryand, P.M., Benidge, B.J., Chao, W.R., and Cummings, J.G.: "Amino Acid Pattern in Uremia: Comparative Effects on Hemodialysis and Transplantation", pp. 405-409, vol. 14, Am. Soc. Art. Int. Organs, (1968).

48. Pitt, W.W., Jr., Scott, C.D., Johnson, W.F., and Jones, G., Jr.: "A Bench-Top Automated, High-Resolution Analyzer for Ultraviolet Absorbing Constituents of Body Fluids", p. 657, vol. 16, Clin. Chem., (1970).

49. Pitt, W.W., Jr., Scott, C.D., and Jones, G., Jr.: "Simultaneous Milticolumn Operation of the UV-Analyzer for Body Fluids", ORNL Pub., Oak Ridge, Tenn., (1972).

50. Pitts, R.F.: "Clearance and Rate of Glomerular Filtration", p. 64, Physiology of the Kidney and Body Fluids, 2nd ed., Year Book Medical Publishers Inc., Chicago, Ill., (1968).

51. Idbid., pp. 228-239.

52. Popovich, R.P., Christopher, T.G., and Babb, A.L.: "The Effects of Membrane Diffusion on Hemodialyzer Design and Performance", pp. 105-115, vol. 67, Chem. Engr. Prog. Sym. Series, (1972).

53. Quadricci, L.J., Cumbi, V., Christopher, T.G., Harker, L.A., and Strider, G.E.: "Assay of Serum Abnormalities in Uremic and Dialysis Patients, Evidence for Depletion of Vital Substances in Hemodialysis", pp. 96-101, vol. 17, Am. Soc. Art. Int. Organs, (1971).

54. Ramirez, W.F., Mickley, M.C., and Lewis, D.W.: "Mathematical Modeling of a Kiil Hemodialyzer", pp. 116-127, vol. 67, Chem. Engr. Prog. Sym. Series, (1972).

55. Ramos, C.P., Christopher, T.G., Maucer, C.J., Scribner, B.H., and Babb, A.L.: "Mass Transfer Resistance Determination of Slowly Dialyzed Molecules with Applications to the pH Dependence of Phosphate Dialysis", pp. 150-153, vol. 16, Am. Soc. Art. Int. Organs, (1970).

56. Richet, G.: "Some Aspects of Uric Acid Metabolism in Chronic Renal Failure", pp. 133-139, Nutrition in Renal Disease, G.M. Berlyne, ed., E. and S. Livingstone, Ltd., Edinburgh, (1968).

57. Schmidt, E.G., McElvain, N.F., and Bowen, J.J.: "Plasma Amino-Acids and the Ether Soluble Phenols in Uremia", pp. 253-261, vol. 20, Am. J. Clin. Path., (1950).

58. Schwerin, P., Bessman, S.P., and Wailsch, H.: "The Uptake of Glutamic Acid and Glutamine by Brain and Other Tissues of the Rat and Mouse", pp. 36-44, vol. 184, J. Biol. Chem., (1950).

59. Scott, C.D.: "Analysis of Urine for Its Ultraviolet-Absorbing Constituents by High-Pressure Anion-Exchange Chromatography", p. 521, vol. 14, Clin. Chem., (1968).

60. Scott, C.D., Attrill, J.E., and Anderson, N.G.: "Automatic High-Resolution Analysis of Urine for Its Ultraviolet-Absorbing Constituents", p. 181, vol. 125, Proc. Soc. Exp. Biol. Med., (1967).

61. Scott, C.D., Chilcote, D.D., and Lee, N.E.: "Coupled Anion and Cation Exchange Chromatography of Complex Biochemical Mixtures", p. 85, vol. 44, Anal. Chem., (1972).

62. Simenhoff, M.L., Asatoor, A.M., Milne, M.D., and Zilva, J.F.: "Retention of Aliphatic Amines in Uremia", pp. 65-77, vol. 25, Clin. Sci., (1963).

63. Sorensen, L.B.: "The Elimination of Uric Acid in Man", pp. 1-214, vol. 12, Suppl. 54, Scan. J. Lab. Invest., (1960).

64. Stein, I.M., Cohen, B.D., and Kornhauser, R.S.: "Guanidino-succinic Acid in Renal Failure, Experimental Azotemia and Inborn Errors of the Urea Cycle", pp. 926-930, vol. 280, New Engl. J. Med., (1969).

65. Stein, I.M. and Micklus, M.J.: "Concentration of Serum and Urinary Excretion of Guanidine, 1-methylguanidine, and 1,1-demethylguanidine in Chronic Renal Failure", pp. 583-585, vol. 19, Clin. Chem., (1973).

66. Stewart, R.D., Lipps, B.J., Baretta, E.D., Piering, W.R., Roth, D.A., and Sargent, J.A.: "Short-Term Hemodialysis with the Capillary Kidney", p. 121, vol. 14, Trans. Am. Soc. Art. Int. Organs, (1968).

67. Susaki, M., Takahara, K., and Natelson, S.: "Urinary Guanidinoacetate/Guanidinosuccinate Ratio: An Indicator of Kidney Disfunction", pp. 315-321, vol. 19, Clin. Chem., (1973).

68. Wolf, A.V., Remp, D.G., Kiley, J.E., and Currie, G.D.: "Artificial Kidney Function: Kinetics of Hemodialysis", p. 1062, vol. 30, J. Clin. Invest., (1951).

69. Young, H.D.: Statistical Treatment of Experimental Data, p. 164, McGraw-Hill Book Co., Inc., (1962).

70. Young, D.S. and Wooton, I.D.P.: "The Retention of Amines as a Factor in Uremic Toxemia", pp. 503-505, vol. 9, Clin. Chim. Acta., (1964).

71. Zarembrski, P.M., Hodgkenson, A., and Parsons, F.M.: "Evaluation of the Concentration of Plasma Oxalic Acid in Renal Failure", pp. 511-512, vol. 212, Nature, (1966).

APPENDIX

Pressure Drop Across the Artificial Kidney

In order to obtain a relation to calculate an expected pressure drop across the CDAK, blood rheology data was obtained (39) at the normal operating ranges for hemodialysis. Since the blood rheology data was reported in wall shear stress versus flow, the pressure drop across the artificial kidney was obtained by

$$(\Delta P)_{calc} = \frac{2\,\tau_w L}{r} \qquad (A1)$$

where $(\Delta P)_{calc}$ = calculated pressure drop across the artificial kidney

τ_w = wall shear stress

L = fiber length

r = fiber radius.

To use equation (A1), it is assumed that (a) blood is a homogeneous, incompressible fluid, (b) laminar, Newtonian flow exists in the fibers, (c) there is no slip at the fiber wall, (d) shear stress depends only on shear rate, and (e) end effects are negligible. The first four assumptions are commonly used (39) for blood flow in capillaries. The last assumption can be checked by calculating the entry length of the fiber required to achieve fully developed flow. For laminar flow,

$$L_e = 0.0575\,(N_{Re})(d) \qquad (A2)$$

where L_e = entry length

N_{Re} = Reynolds number

d = fiber diameter.

For a blood flow rate of 300 ml/min, the entry length calculated from equation (A2) is 0.016 cm which is negligible to the total fiber length of 16 cm. This shows that assumption (e) is valid. The blood rheology data in Table A1 was used to obtain an empirical relation between $(\Delta P)_{calc}$, blood flow rate, and hematocrit. Table A2 can now be developed by performing a linear regression analysis on HCT versus $\ell n(\Delta P)_{calc}$ at each blood flow rate. Performing a linear regression analysis on $\ell n(Q_B)$ versus m and $\ell n(Q_B)$ versus b, the final empirical relation for the pressure drop across the artificial kidney is

$$(\Delta P)_{calc} = (f)\exp[(-7.187\times10^{-3}\ell n Q_B+0.0804)(HCT)+1.137\ell n Q_B-3.753] \quad (A3)$$

where f = unity with units of (mm Hg)

Q_B = blood flow rate (ml/min)

HCT = hematocrit (vol%).

Equation (A3) was obtained by empirical data and can be used for blood flow rates ranging from 100 ml/min to 300 ml/min and for hematocrits ranging from 15 vol% to 35 vol%.

TABLE A1

REPORTED BLOOD RHEOLOGY DATA FOR CAPILLARY FLOW (39)

HCT (vol %)	ΔP_{100} (mm Hg)	ΔP_{150} (mm Hg)	ΔP_{200} (mm Hg)	ΔP_{250} (mm Hg)	ΔP_{300} (mm Hg)
15	9.3	14.3	19.0	24.2	29.2
25	13.3	19.3	25.0	31.5	35.5
33	22.4	31.9	41.0	50.9	60.5
35	23.1	32.7	43.0	52.0	61.6

ΔP_{100} = pressure drop at a blood flow rate of 100 ml/min

ΔP_{150} = pressure drop at a blood flow rate of 150 ml/min

ΔP_{200} = pressure drop at a blood flow rate of 200 ml/min

ΔP_{250} = pressure drop at a blood flow rate of 250 ml/min

ΔP_{300} = pressure drop at a blood flow rate of 300 ml/min

HCT = blood hematocrit

TABLE A2

REGRESSION ANALYSIS OF THE DATA IN TABLE A1

Blood Flow Rate (ml/min)	m	b
100	0.0477	1.478
150	0.0437	1.962
200	0.0428	2.251
250	0.0403	2.541
300	0.0398	2.727

m = slope from the regression analysis of HCT versus $\ln(\Delta P)$

b = intercept from the regression analysis of HCT versus $\ln(\Delta P)$